DOCUMENT CLOSED

Climate change enhanced intensity of Hurricane Melissa, testing limits of adaptation in Jamaica and eastern Cuba

Authors

Ben Clarke, *Centre for Environmental Policy, Imperial College, London, UK*
Clair Barnes, *Centre for Environmental Policy, Imperial College, London, UK*
Theodore Keeping, *Centre for Environmental Policy, Imperial College, London, UK*
Nathan Sparks, *Department of Physics, Imperial College, London, UK*
King Heng Lau, *Department of Physics, Imperial College, London, UK*
Ralf Toumi, *Department of Physics, Imperial College, London, UK*
Maja Vahlberg, *Red Cross Red Crescent Climate Centre, The Hague, the Netherlands (based in Ubmeje/Umeå, Sweden)*
Roop Singh, *Red Cross Red Crescent Climate Centre, The Hague, The Netherlands (based in New Jersey, USA)*
Julie Arrighi, *Red Cross Red Crescent Climate Centre, The Hague, The Netherlands; Global Disaster Preparedness Centre, American Red Cross, Washington D.C., USA; Tufts University, Boston, USA (based in New York, USA)*
Cornelia Scholz, *Red Cross Red Crescent Climate Centre, The Hague, The Netherlands (based in Vienna, Austria)*
Nick Baumgart, *Copenhagen Centre for Disaster Research, Department of Public Health, University of Copenhagen*
Emmanuel Raju, *Copenhagen Centre for Disaster Research, Department of Public Health, University of Copenhagen*
Michael A. Taylor, *Department of Physics, The University of the West Indies, Mona, Jamaica*
Tannecia S. Stephenson, *Department of Physics, The University of the West Indies, Mona, Jamaica*
Jhordanne J. Jones, *Department of Physics, The University of the West Indies, Mona, Jamaica*
Jayaka D. Campbell, *Department of Physics, The University of the West Indies, Mona, Jamaica*
Jacqueline M. Spence, *Meteorological Service, Jamaica*
Abel Centella-Artola, *Institute of Meteorology, La Habana, Cuba*
Arnoldo Bezanilla-Morlot, *Institute of Meteorology, La Habana, Cuba*
José Rubiera, *Forecast Center, Institute of Meteorology, Cuba*
Claire Bergin, *ICARUS Climate Research Centre, Maynooth University, Maynooth, Ireland*
Wenchang Yang, *Department of Geosciences, Princeton University, Princeton, NJ, USA*
Friederike Otto, *Centre for Environmental Policy, Imperial College, London, UK*

Review authors

Sjoukje Philip, *Royal Netherlands Meteorological Institute (KNMI), De Bilt, The Netherlands*
Sarah Kew, *Royal Netherlands Meteorological Institute (KNMI), De Bilt, The Netherlands*
Dora Vrkić, *Grantham Institute - Climate Change and the Environment, Imperial College London, London, UK*

Cite as Clarke, B. et al., (2025): Climate change enhanced intensity of Hurricane Melissa, testing limits of adaptation in Jamaica and eastern Cuba (WWA scientific report No. 76) World Weather Attribution DOI: 10.25560/125306

Main findings

- Hurricane Melissa moved very slowly across the Caribbean, allowing the storm to gather immense destructive energy over very warm ocean waters. When it finally made landfall in Jamaica as a Category 5 hurricane, the storm hit a region familiar with hurricanes but unaccustomed to one of such exceptional strength and intensity.

- With more than 2.6 million Jamaicans and 3.8 million Cubans exposed to extremely strong winds (fig. 1a), the storm has severely damaged critical infrastructure such as telecommunications, roads, hospitals and disrupted water systems, adding challenges to immediate response as well as long-term recovery.

- The heavy rainfall from Hurricane Melissa also impacted neighboring countries, including the Dominican Republic, Cuba, and the highly vulnerable nation of Haiti. Haiti experienced significant, localised flooding and at least 31 deaths driven, in part, by the ongoing severe humanitarian crisis and related population vulnerabilities.

- To estimate if human-induced climate change influenced the heavy rainfall, we first determine if there is a trend in the observations. In Jamaica, we find that heavy 5-day rainfall events such as the one associated with Melissa are about 30% more intense and about twice as likely in today's climate, that is 1.3°C warmer than it would have been without human-induced climate change. In Eastern Cuba the observations show an even stronger increase of about 50% in intensity and a factor 9 in frequency.

- To determine the role of climate change in the rainfall, we combine observations with climate models. We find that climate models are not able to represent the observed trends and underestimate the extreme rainfall. This is a known problem in the Caribbean and is in part because many climate models have relatively coarse spatial resolution, meaning they do not accurately capture the most intense tropical cyclone rainfall over small islands. In addition, the IRIS model was used to investigate the rainfall rate in Melissa's eye wall, finding an increase in likelihood of 43% and about 16% in intensity of the rainfall associated with a storm like Melissa.

- Taking all lines of evidence together, including the observations, the IRIS analysis, other studies in the region, and physical reasoning, that in a warming climate an increase in heavy rainfall is expected, we estimate an increase in intensity of the rainfall associated with hurricanes like Melissa to be larger than 9%.

- The IRIS model was also used to investigate Melissa's strong winds by analysing storms making landfall in the same region as Melissa. By statistically simulating these storms in a 1.3°C cooler climate, this model showed that climate change was responsible for an increase in frequency by a factor of about 5 in the number of such storms (now once every 1700 years on average, up from every 8100 years), and equivalently that the maximum wind speeds of similar storms are now about 5.1 m/s (around 7%) more intense. Increases in wind speed lead to an exponential increase in damages.

- The sea surface and atmospheric conditions leading to a storm's intensity were also studied – using a metric known as *potential intensity.* We find that long-term, natural variability in the climate (represented by the Atlantic Multidecadal Variability in our analysis) explains about 43% of the variability of the potential intensity in the Caribbean. Independent of this internal climate variability, hurricane-conducive conditions are becoming more intense as the planet warms. We find that climate change increased the likelihood of conditions as extreme as those observed in October 2025 by a factor of about 6.

- Despite the Caribbean's high exposure to intense hurricanes, and having contributed very little to global warming, globally available data and climate models do not capture the climate of the Caribbean well and require more investment and attention.

- Our results are consistent with other recently published rapid analyses (Climameter, Climate Damage Tracker, Climate Central). While each of these studies used different methodologies and addressed different research questions, the overarching finding is that climate change is enhancing conditions conducive to the most powerful hurricanes like Melissa, with more intense rainfall and wind speeds, leading to more destructive storms, causing high human and economic impacts.

- Hurricane Melissa struck a year after Hurricane Beryl made landfall in the same region, devastating agriculture and fishery communities and further damaging infrastructure that had not yet recovered.

- Jamaica, like many small island states, faces potentially catastrophic economic losses from hurricanes. To mitigate such risks, the government employs a multi-layer financial strategy, including disaster risk insurance, catastrophe bonds, parametric insurance

through the Caribbean Catastrophe Risk Insurance Facility (CCRIF), and pre-arranged lines of credit with the World Bank and Inter-American Development Bank. For instance, a US$150 million catastrophe bond is expected to fully pay out after Hurricane Melissa. Despite these measures, preliminary estimates suggest damages from Melissa are at least an order of magnitude larger than available finance, representing a proportion of GDP or even a factor of GDP, posing a huge strain on the country. Further, there are psycho-social and other nonfinancial impacts that are not easily quantified or included in these figures, but require acute attention.

- In both Jamaica and Cuba, forecasts of Melissa were available at least 7 days before landfall, with steadily increasing certainty on the track, strength, and timing of potential impacts, providing adequate lead time for preparation. In Cuba this led to the evacuation of more than 735,000 people in low lying and coastal areas. In Jamaica, this allowed for the opening of 881 emergency shelters, evacuations of people in the direct path, pre-positioning of emergency supplies, the closure of airports and diversion of cruise ships. These efforts likely saved many lives. While additional adaptation efforts could be made, with such an intense storm we cannot reasonably expect preparedness actions to have averted all impacts, as the storm tests some of the soft limits to adaptation, especially with regards to infrastructure.

1 Introduction

Early on October 28th, Hurricane Melissa made landfall on the southern coast of Jamaica as a Category 5 storm on the Saffir-Simpson scale, generating high winds, extreme rainfall and storm surges in coastal areas. The following day, it weakened to Category 3 before impacting Cuba and the extremely vulnerable Haiti, bringing strong winds, storm surges and heavy rainfall.

It will take weeks for the full extent of the damages to be known, as Melissa has caused widespread damage and disruption to critical infrastructure, including washed out roads, damaged water supply, power outages and communication disruption. The hurricane also damaged weather monitoring systems, posing further challenges to accurately estimating the total rainfall and the breadth of its impacts.

At least 28 people have been confirmed dead in Jamaica at the time of writing (Jamaica Gleaner, 2025), with at least another 31 fatalities reported in Haiti and two confirmed deaths in the Dominican Republic (BBC, 2025), leading to a total of 61 deaths (as of 4th November 2025) across the affected Caribbean islands.

Aside from destroying the infrastructure and homes, Melissa also caused widespread damage to crops. Melissa has and will continue to have severe impacts on people's livelihoods, particularly in agriculture, fishing, and tourism. In Jamaica, on top of significant damages to hotels and tourism

infrastructure, Melissa heavily impacted or destroyed agricultural areas such as St. Elizabeth - known as the country's breadbasket - and remote fishing communities such as White House (BBC, 2025, CNN, 2025). In Haiti and Cuba, fields were submerged and livestock washed away (Tageschau, 2025, Washington Post, 2025). Agriculture and tourism are important pillars of Jamaica's, Cuba's, and Haiti's economies, affecting local economies and exports broadly, requiring extensive recovery (Hidalgo et al., 2025, USDA, 2024, UN Stats, 2023).

Melissa formed as a tropical storm on 21 October, from a centre of organised deep convection that had been monitored by the National Hurricane Centre from 19 October onwards (NHC, 2025). Melissa initially moved slowly (between 1-3 mph) and erratically west to northwest across the very warm waters of the central Caribbean after forming (Fig.1.1). However, strong westerly wind shear prevented the storm from strengthening significantly during this early stage. By October 23, the wind shear began to ease, allowing new convection to develop downshear from the storm's center. As Melissa became better aligned vertically, it started to turn more northward and gradually intensified the following day.

With environmental conditions becoming highly favorable, Melissa entered a period of rapid intensification on October 25, with maximum sustained winds increasing from 70 mph (115 km/h) to 140 mph (225 km/h) in just 18 hours (Scientific American, 2025). After a brief pause, strengthening resumed, and while moving generally westward, Melissa reached Category 5 status early on October 27, gaining energy from the unusually warm ocean temperatures (Climate Central, 2025; Fig. 1.1). The storm then turned north-northeastward and continued to intensify, reaching peak winds of 185 mph (295 km/h). At 17:00 UTC, Melissa made landfall near New Hope in Westmoreland Parish at its peak intensity.

According to Met Service bulletins issued near the time of landfall, hurricane-force winds associated with Melissa extended outward up to 30 miles (≈ 45 km) from the storm's eye, while tropical-storm-force winds reached as far as 195 miles (≈ 315 km) from the centre (Jamaica Observer, 2025; National Hurricane Center, 2025). Given that Jamaica measures approximately 235 km (146 miles) long and up to 80 km (50 miles) wide, hurricane-force winds would have affected roughly a third of the island lengthwise, covering all of the western and most central parishes. Tropical-storm-force winds, by contrast, encompassed the entire island and extended well beyond its borders, explaining why Melissa's impact was felt nationwide rather than regionally.

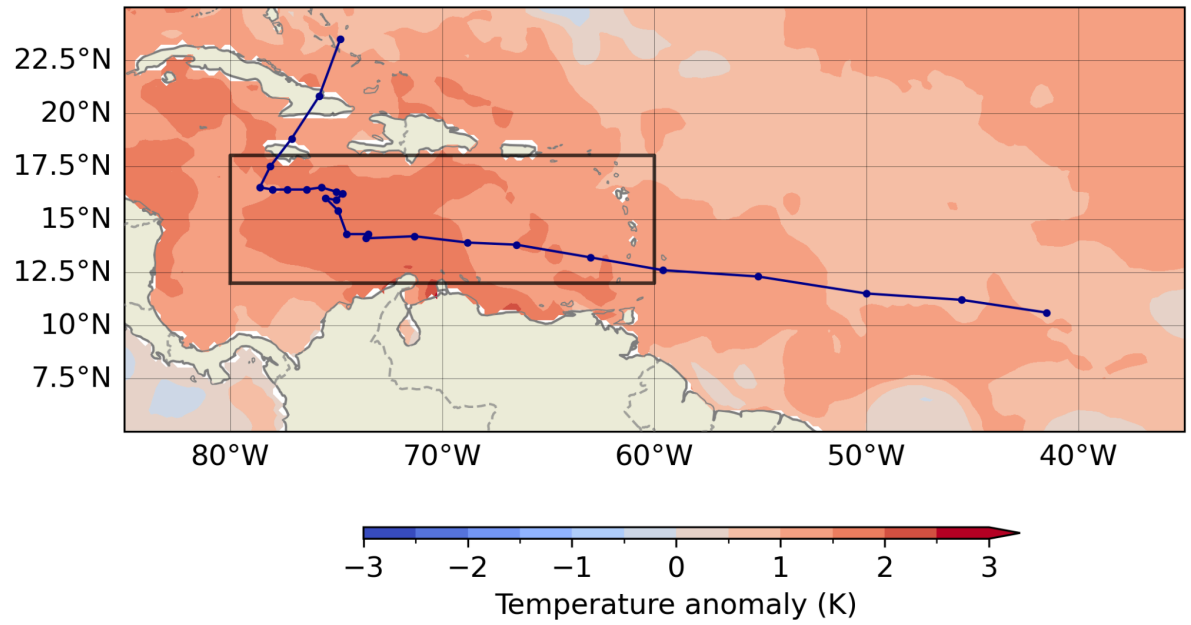

Figure 1.1: *October sea surface temperatures anomalies over the Caribbean and western Atlantic. Anomalies are calculated for October 2025 with respect to July-December in the period 1991-2020. The track of Hurricane Melissa is shown as a series of dark blue points, and the black region is used for potential intensity analysis in section 3 of this report. The average anomaly over the region was 1.45°C. Data from ERA5.*

1.1 Hurricanes in the Caribbean

The North Atlantic (NA) hurricane season lasts from June-November and overlaps with the early (May-June) and late rainfall seasons (September-November) in the main Caribbean basin. During this time of the year, weak easterly trade winds, decreased vertical wind shear, and sea surface temperatures in excess of 26°C characterize the Caribbean (Climate Studies Group Mona 2020). The NA hurricane season is most active from mid-August to late October, with September showing peak activity. The Caribbean has been impacted by several major hurricanes. Some notable tropical cyclones (TCs) in recent times include category 5 Hurricanes Irma and Maria in 2017; Dorian in 2019; and Beryl in 2024.

Irma, one of the longest-lasting hurricanes on record (30 August - 12 September), made landfall in Barbuda, St. Martin, British Virgin Islands, Bahamas, Cuba, Florida Keys and south Florida. Irma caused 47 direct deaths as a result of its strong winds, heavy rains, and high surf across the Caribbean Islands and the southeastern United States (NHC 2021) and caused immense property damage estimated at US$64-90 billion (Metych 2025). Maria (16 - 30 September) made landfall in Dominica and Puerto Rico causing 31 (direct) and 2975 (direct and indirect) deaths respectively (Pasch et al. 2023, Payne 2025). The losses in Dominica equaled 226% of its GDP and the costs for repairs for Puerto Rico is estimated at US$115 billion (Payne 2025, World Bank 2018). Hurricane Dorian (24 August - 7 September 2019) was one of the strongest hurricanes to hit the Bahamas (particularly Abaco and Grand Bahama). Dorian resulted in approximately 74 deaths and estimated damages and losses of US$3.4 billion (IDB 2020, IFRC 2023). Hurricane Beryl (28 June - 9 July 2024) was an early-season major hurricane that showed rapid intensification and made landfall in the Carriacou

Island, Grenada; Yucatan Peninsula of Mexico; and Texas, and also caused severe impacts in St. Vincent and the Grenadines, and Jamaica. Beryl caused at least 69 deaths with 35 of these directly attributed to the cyclone's winds, rains, and tornadoes (NHC 2025).

Prior to Hurricane Melissa, the more recent hurricanes making landfall in Jamaica include Hurricane Charlie in 1951 and Hurricane Gilbert in 1988, both at category 3. These TCs resulted in 152 and 45 deaths respectively, with Charlie linked to losses of US$50 million in comparison to Gilbert at US$4 billion (Gleaner 2021, Gleaner 2024). Some other notable storms impacting Jamaica, though not making landfall, include cat. 4 Hurricane Ivan in 2004 which was linked to 31 (direct and indirect) deaths and losses of JMD$36.8 billion (US$580 million), and cat. 4 Hurricane Dean in 2007 linked to 3 deaths and losses of JMD$23.8 billion (US$300 million) (PIOJ 2004, NHC 2008, Jamaica Observer 2024, Gleaner 2025). Beryl was the last major storm traversing close to Jamaica. The storm resulted in 4 deaths and JMD$32.2 billion loss (Gleaner 2025). The eye wall of the system hit southern parishes causing major structural damage in sections of Clarendon, Manchester, and St Elizabeth, the last two being the most severely affected (Gleaner 2025).

The influence of climate change on TCs varies by basin, as does the level of scientific evidence on these changes (Masson-Delmotte et al., 2021). On a global scale, recent decades have seen an increase in more intense TCs (category 3-5 on the Saffir-Simpson scale), but no change in the overall number of TCs. Recent studies on specific TCs as well as physical understanding suggest that extreme rainfall from TCs is increasing (Masson-Delmotte et al., 2021). This is explained partly by the Clausius-Clapeyron relation, which states that warmer air holds more moisture at a rate of 6-7% / °C. In the future, the proportion of the most intense TCs (categories 4-5) is projected to increase with further warming, as well as the average and maximum precipitation rates from these storms (Seneviratne et al., 2021).

Basin-specific changes are less certain, more variable and extend to other properties of TCs. For instance, in the NA, TCs making landfall over the contiguous US have slower translation speeds (Kossin, 2019) and are more frequently stalling or meandering, leading to more intense impacts as extreme conditions are sustained for longer periods over a given location (Seneviratne et al., 2021). In addition, NA hurricanes are increasing in both intensification rate and maximum intensity, which is unlikely to be explained by natural variability (Bhatia et al., 2019; Murakami et al., 2020).

Attribution studies now provide additional insight into the changing nature of hurricanes in a warming world. Hurricanes in the NA basin are the most frequently studied tropical cyclone events to date, with studies covering 10 recent events with combined damages of more than US$700 billion (at the time of occurrence) in the US and Caribbean. Almost across the board, rainfall from these events were amplified by anthropogenic climate change: Katrina in 2005 by 4%, Irma in 2017 by 6%, Maria in 2017 by 9% (Patricola and Wehner, 2018), Florence in 2018 by 5% (Reed et al., 2020), Dorian in 2019 by 5-18% (Reed et al., 2021), Ian in 2022 by 18% (Reed et al., 2023), Harvey in 2017 by 7-38%, and Helene and Milton by approximately 10% (Clarke et al., 2024a; Clarke et al., 2024b).

Changes in wind intensity are generally less clear than for rainfall, though recently developed methods have detected widespread attributable increases in the winds speeds of recent events. One study using a pseudo global-warming approach found no detectable change in intensity to date but projected significantly increasing intensity at higher warming levels (Patricola and Wehner, 2018), while a rapid study found that the winds due to Helene had become approximately 6 m/s more intense

due to anthropogenic warming (Clarke et al., 2024a). Furthermore, recent studies by Climate Central showed that all recent hurricanes from 2019-2024 were intensified by anthropogenic warming (Gilford et al., 2024; Climate Central, 2024). Finally, while attributable effects on storm surge are rarely analysed, one study showed that during Hurricane Sandy in 2012, the effect of sea level rise due to climate change created a higher storm surge, directly leading to an additional US$8.1 billion in damages (Strauss et al., 2021).

As part of this basin, the Caribbean is facing and will continue to face growing hurricane hazards in a warming world, but has historically received far less attention than the mainland US (Vosper et al., 2020). Hurricane Melissa highlights both the urgency of these problems and the imperative for greater understanding of risks in this region.

1.2 Event Definition(s)

In this study, we characterise Hurricane Melissa in several ways in order to capture both the environmental conditions leading to its intensity and the range of ways in which it led to impacts, including both extreme rainfall and high winds. This follows similar methodology as recent rapid studies on Typhoon Gaemi and Hurricane Helene (Clarke et al., 2024a; Clarke et al., 2024c). The results of the analyses are split into three sections, and all data and methods are described in the appendices (A.1).

First, the WWA probabilistic event attribution protocol (Philip et al., 2020; van Oldenborgh et al., 2021) is applied to extreme rainfall across the affected region where impacts were reported. This is divided into four sections to reflect the rainfall driven impacts experienced in different regions; Jamaica, eastern Cuba, southern Haiti and southern Dominican Republic. This analysis gives a probabilistic analysis of both precipitation extremes using a synthesis of observational and climate model products for Jamaica and eastern Cuba, while trends in southern Haiti and southern Dominican Republic are explored in observations only. The hurricane season in the Caribbean runs from June-November, but the period of highest activity overlaps with the Caribbean's primary wet season (September-November). Therefore, extremes occurring during September-November were analysed to capture those events of similar character to Melissa. The influence of this choice on the results is small (see section A.2.1). The rainfall event definitions are as follows:

Rainfall:

- **Jamaica:** September-November maximum 5-day accumulations of area-averaged precipitation over the island of Jamaica
- **Eastern Cuba:** September-November maximum 5-day accumulations of area-averaged precipitation over land areas in Cuba east of 78 °W
- **Dominican Republic:** September-November maximum 5-day accumulations of area-averaged precipitation over land areas in the Dominican Republic south of 18.7 °N
- **Haiti:** September-November maximum 5-day accumulations of area-averaged precipitation over land areas in Haiti south of 18.7 °W

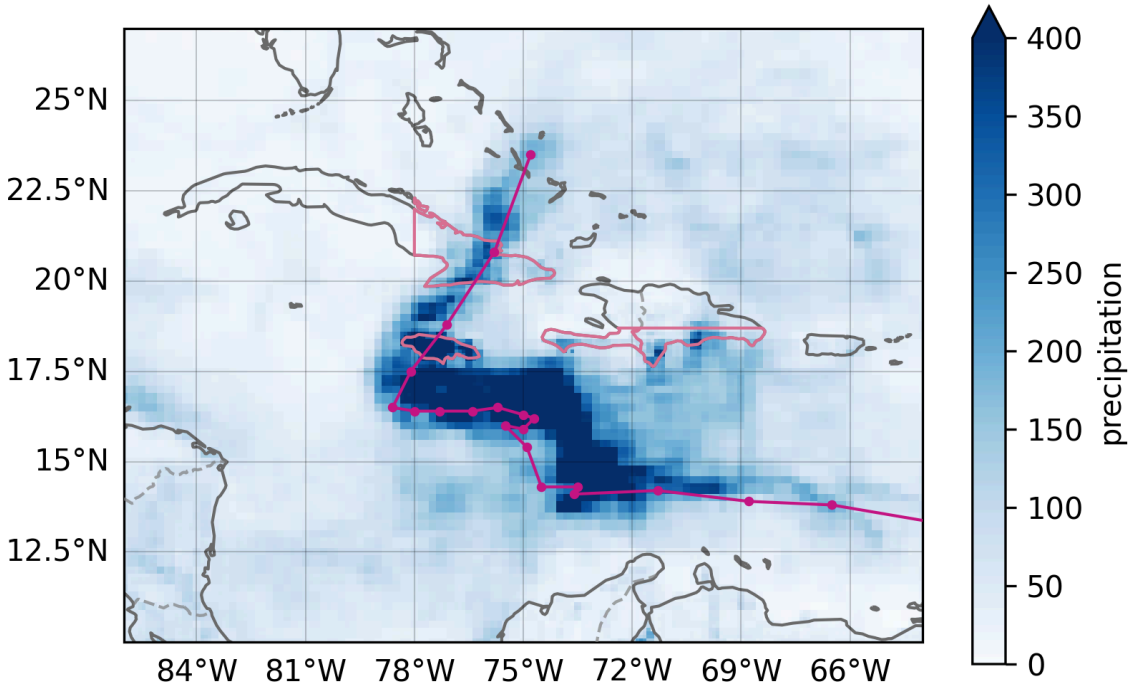

Figure 1.2: *The wettest 5-day period in each location between 19-29 October 2025, which is clearly related to the passage of Melissa. Note that, for the event definitions, daily precipitation is first averaged over the study domains and then the maximum 5-day accumulation is determined, whereas in Figure 1.2 the dates of the wettest 5-day periods within a study region, e.g. Haiti, may slightly differ. The track of Hurricane Melissa at 12 hour intervals is shown as a series of pink points, and the pink regions are those used for extreme rainfall analysis in section 2 of this report. Data from MSWX.*

Second, we characterise the conditions that led to such an event using the potential intensity. This metric predicts maximum hurricane wind speeds by combining sea surface temperatures, sea level pressure, and temperature and humidity vertical profiles (Pérez-Alarcón et al., 2023; Emanuel, 1986). The potential intensity observed during the month of October 2025 is analysed in section 3 using the WWA method.

Environmental conditions:

1. **Peak potential intensity (PI) in the Caribbean:** annual maxima of monthly potential intensity averaged over the sea surface from 80-60 °W, 12-18 °N (figure 1.3)

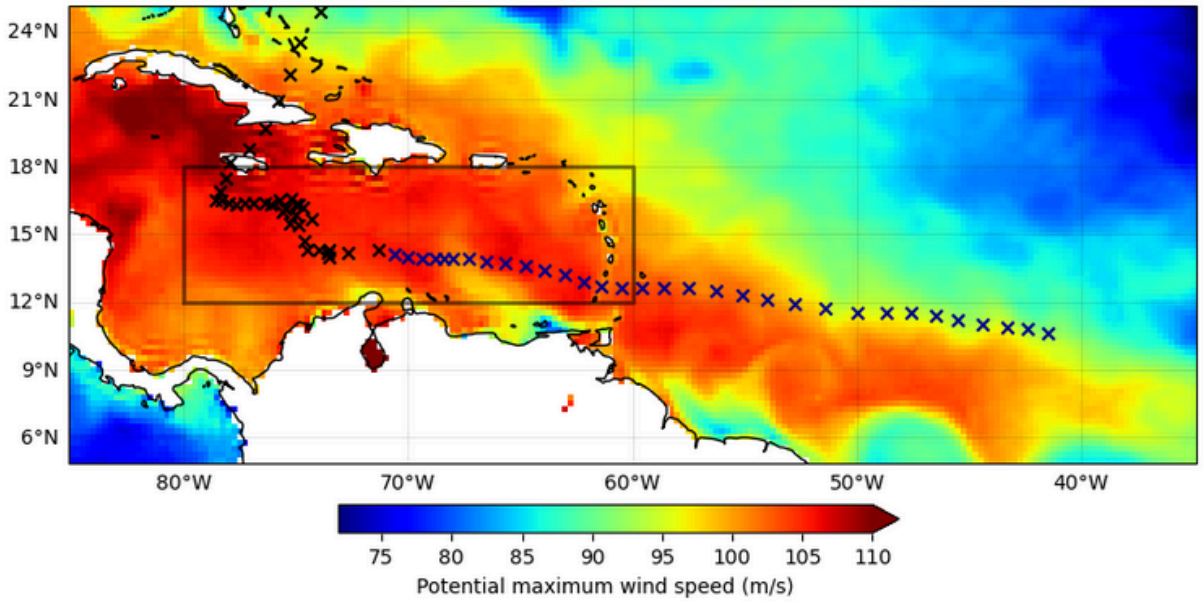

Figure 1.3: *October (1st-27th) mean potential intensity in the Caribbean sea, Gulf of Mexico and western Atlantic. The study region is shown by the black box and the track of Melissa is shown as crosses. Data from ERA5.*

Finally, in section 4, the attributable changes in both wind speed intensity and rainfall are assessed using IRIS, a stochastic model of storm tracks and intensities.

IRIS:

1. **Rainfall:** eyewall rainfall rate from hurricanes making landfall on Jamaica
2. **Wind speed:** wind speed of hurricanes making landfall on Jamaica with a maximum sustained wind speed of at least 80 m/s immediately prior to landfall (figure 1.4)

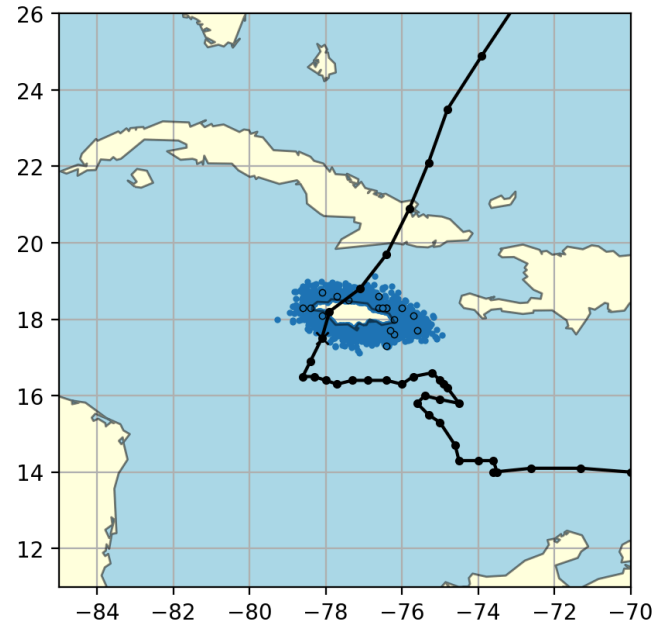

Figure 1.4: *Samples drawn from the IRIS dataset (blue dots) and historical landfall events in Jamaica (black circles). The track of Melissa is shown in black.*

For each event definition, we study the influence of anthropogenic climate change by comparing the likelihood and intensity of similar events at present with those in a 1.3°C cooler climate. For the rainfall and potential intensity, we also extend this analysis into the future by assessing the influence of a further 1.3°C of global warming from the present. This is in line with the latest Emissions Gap Report from the United Nations Environment Programme, which shows that the world is on track for at least 2.6°C temperature rise given currently implemented policies (UNEP, 2024).

2. Extreme rainfall attribution using WWA protocol

The event definitions studied in this section are as follows:

- **Jamaica:** September-November maximum 5-day accumulations over the island of Jamaica (figure 1.2)
- **Eastern Cuba:** September-November maximum 5-day accumulations over land areas in Cuba east of 78 °W (figure 1.2)
- **Dominican Republic:** September-November maximum 5-day accumulations over land areas in the Dominican Republic south of 18.7 °N (figure 1.2)
- **Haiti:** September-November maximum 5-day accumulations over land areas in Haiti south of 18.7 °W (figure 1.2)

The data and statistical modelling used in this section are described in appendix A.1.

2.1 Observational analysis

In this subsection, a nonstationary GEV is fit to the time series of each extreme index from each observational dataset, which scales with GMST. This enables estimation of the return periods in the present day for an event of the magnitude observed during the passage of Hurricane Melissa (tables 2.1-2.4). There is strong variation between regions in how extreme the rainfall was, though all return period estimates use only a single gridded reanalysis product (MSWX) available at the time of the analysis. At the time of writing, widespread station-based observations of the event are not yet available, though preliminary data for Cuba from 23rd - 28th October, along with a comparison to MSWX, is shown in appendix A.1.1.

In addition to using a single covariate of GMST, we also tested the influence of two additional covariates (see appendix A.1 for a description of the statistical methods). Global climate modes could also have a substantial effect on hurricane occurrence and rainfall patterns in the Atlantic. First, the multidecadal Atlantic Multidecadal Variability (AMV), a very long period apparent oscillation in north Atlantic mean sea surface temperatures, has been linked to variability in wind shear conditions affecting tropical Atlantic hurricane formation (Knight et al., 2006) and hurricane-related extreme rainfall (Curtis, 2008). The index calculation is described in Section A.1. Second, an SST gradient between the tropical Pacific and Atlantic oceans, represented by the difference between the Nino3 (bounded by 6 °S - 6 °N, 150 °W - 90 °W) and Tropical North Atlantic (bounded by 6 °S - 22 °N, 80 °W - 15 °W) sea surface temperatures, is known to influence precipitation in the region (Taylor et al., 2002). These additions did not significantly and consistently improve the fit to the time series of precipitation extremes in different regions when also accounting for the increased complexity of the model (by the Akaike Information Criterion). Consequently, GMST is used as the only covariate in this analysis, but the potential role of these drivers in similar extremes also warrants further exploration.

In Jamaica, the 5-day rainfall (Rx5Day) was estimated as a 40-year return period event under current climate conditions (table 2.1), which is very similar to that for the 2-day accumulation (see appendix A.2.2.1). In eastern Cuba, the 5-day rainfall was estimated as a ~10-year return period event under current climate conditions (table 2.2), which is also very similar to that for the 2-day accumulation

(see appendix A.2.2.2). In southern Haiti and the Dominican Republic, the 5-day event was relatively common, with return periods of ~2 and ~6 years, respectively. The return periods are similar when averaging across the wider country in each case (see appendices A.2.2.3 & A.2.2.4). The intense rains that ultimately led to known impacts likely occurred on very localised scales that are not captured with a regional average, and also combined with local vulnerabilities to cause these impacts (section 6).

Dataset	Jamaica 5-day rainfall		Trend with GMST	
	Magnitude (mm)	Return period (95% C.I.)	Probability Ratio (95% C.I.)	Change in magnitude (95% C.I.) (%)
MSWX	519.7	39.0 (13.3 to 343.0)	**3.52 (1.24 to 15.8)**	**63.8 (7.59 to 133)**
CHIRPS	358	40 (15.9 to 2890)	1.47 (0.013 to 94.4)	11.2 (-56.4 to 75.8)

Table 2.1: *Observed magnitude and estimated return period in current climate conditions for the 5-day rainfall associated with Melissa in MSWX, and the corresponding magnitude for a 40-year return period event in CHIRPS. Change in probability ratio and magnitude for Rx5Day in Jamaica with increasing GMST are also shown.* ***Bold text*** *indicates a statistically significant (at the 95% confidence level) increasing trend.*

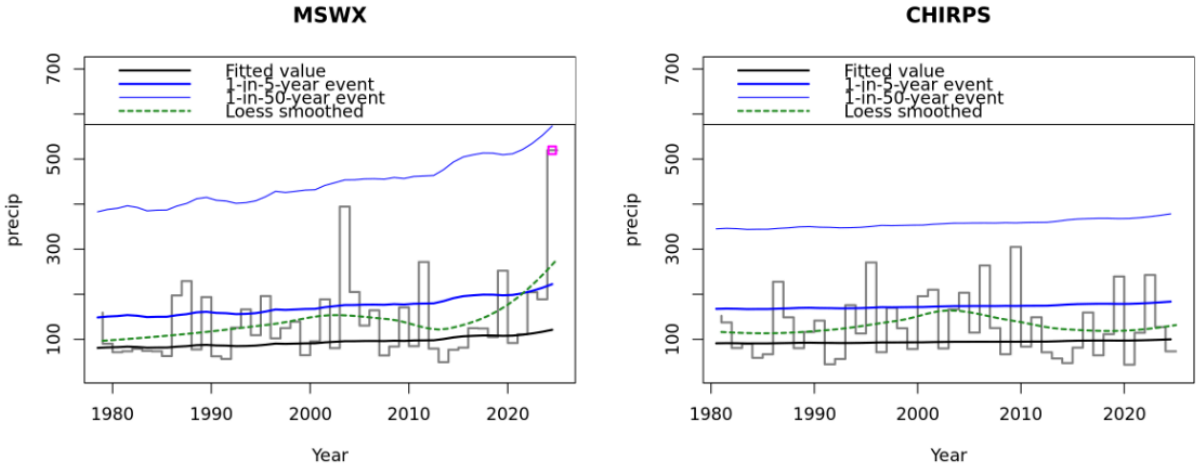

Figure 2.1: *Time series of September-November maxima of 5-day accumulated precipitation in Jamaica in MSWX (left) and CHIRPS (right). The modelled influence of GMST on the expected value (5- and 50-year return period values) is shown with the black line (bold and lighter blue lines), while the loess smoothed trend is shown with the green dashed line. The purple box shows the magnitude of the observed event in MSWX (left).*

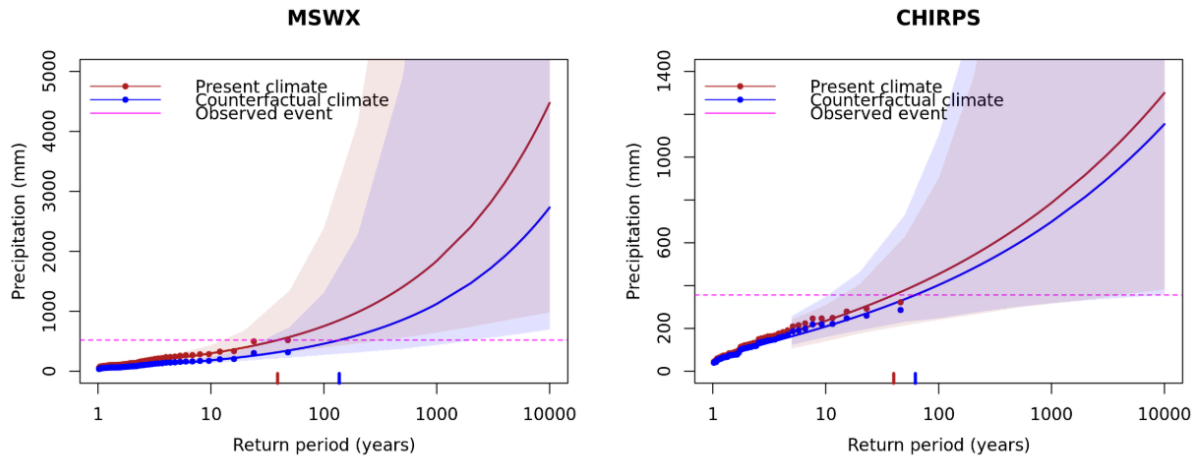

Figure 2.2: *Statistical fits to September-November maxima of 5-day accumulated precipitation in Jamaica, in MSWX (left) and CHIRPS (right). The influence of GMST is shown with the red vs blue probability curves. The magnitude of the event is highlighted with a horizontal purple line.*

Dataset	Eastern Cuba 5-day rainfall		Trend with GMST	
	Magnitude (mm)	Return period (95% C.I.)	Probability Ratio (95% C.I.)	Change in magnitude (95% C.I.) (%)
MSWX	148	8.77 (3.53 to 31.0)	9.43 (0.59 to inf)	54.8 (-22.9 to 125)
CHIRPS	167	10 (4.10 to 91.1)	7.10 (0.445 to 253)	52.7 (-14.9 to 184)

Table 2.2: *Observed magnitude and estimated return period in current climate conditions for the 5-day rainfall associated with Melissa in MSWX, and the corresponding magnitude for a 10-year return period event in CHIRPS. Change in probability ratio and magnitude for Rx5Day in eastern Cuba with increasing GMST.*

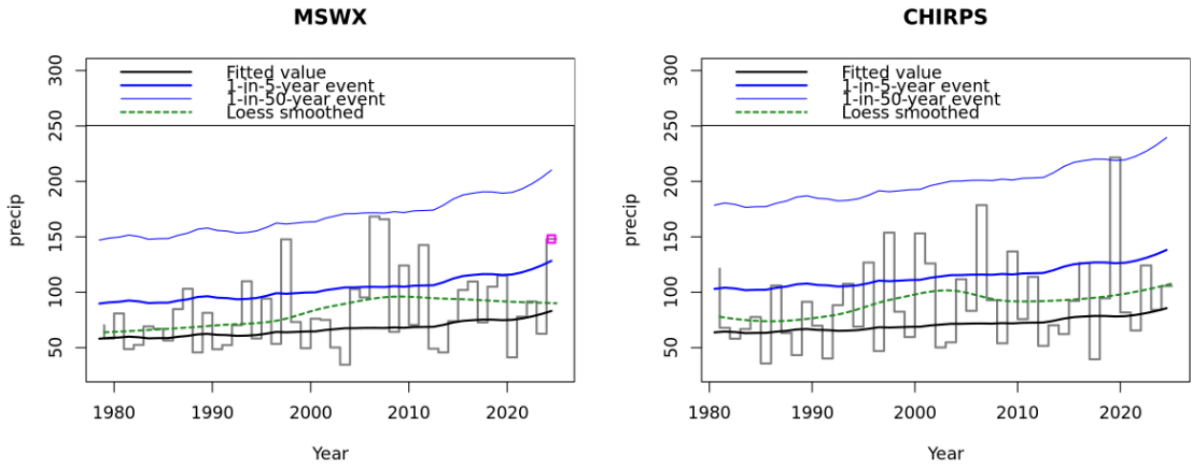

Figure 2.3: *Time series of September-November maxima of 5-day accumulated precipitation in the eastern region of Cuba affected by Hurricane Melissa, in MSWX (left) and CHIRPS (right). The*

modelled influence of GMST on the expected value (5- and 50-year return period values) is shown with the black line (bold and lighter blue lines), while the loess smoothed trend is shown with the green dashed line. The purple box shows the magnitude of the observed event in MSWX (left).

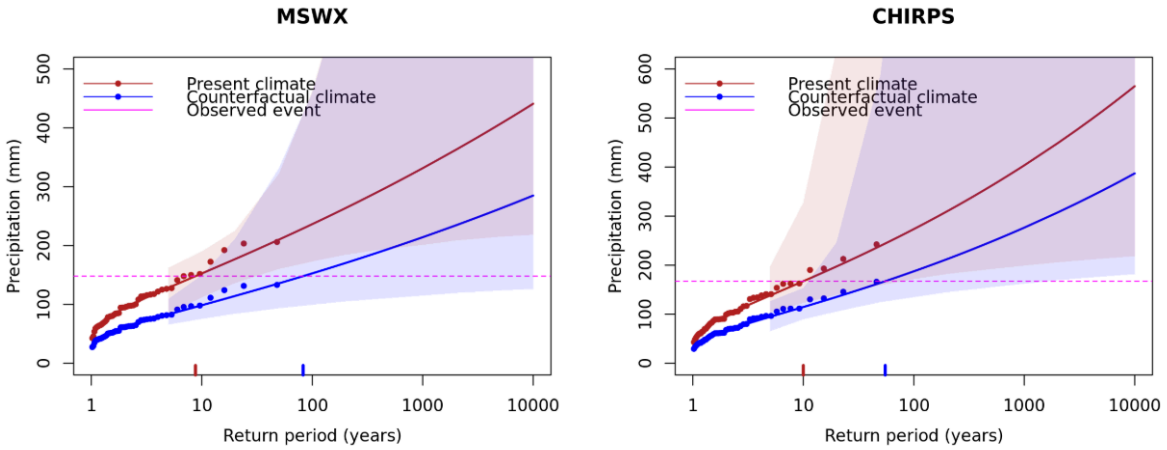

Figure 2.4: *Statistical fits to September-November maxima of 5-day accumulated precipitation in eastern Cuba, in MSWX (left) and CHIRPS (right). The influence of GMST is shown with the red vs blue probability curves. The magnitude of the event is highlighted with a horizontal purple line.*

Dataset	Haiti 5-day rainfall		Trend with GMST	
	Magnitude (mm)	Return period (95% C.I.)	Probability Ratio	Change in magnitude (%)
MSWX	99.9	2.12 (1.33 to 3.60)	1.25 (0.62 to 2.74)	15.8 (-28.2 to 86.3)
CHIRPS	104.5	2	1.06 (0.26 to 3.00)	2.80 (-41.8 to 70.3)

Table 2.3: *Observed magnitude and estimated return period in current climate conditions for the 5-day rainfall associated with Melissa in MSWX, and the corresponding magnitude for a 2-year return period event in CHIRPS. Change in probability ratio and magnitude for Rx5Day in southern Haiti with increasing GMST. Trends close to 'no change' (change in intensity <5%) are highlighted in grey.*

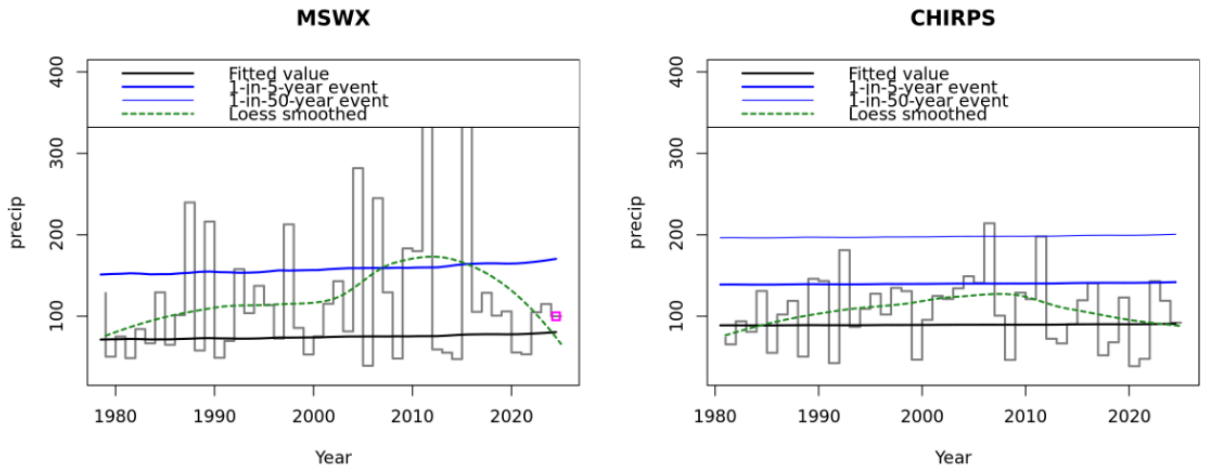

Figure 2.5: *Time series of September-November maxima of 5-day accumulated precipitation in the southern region of Haiti affected by Hurricane Melissa, in MSWX (left) and CHIRPS (right). The modelled influence of GMST on the expected value (5- and 50-year return period values) is shown with the black line (bold and lighter blue lines), while the loess smoothed trend is shown with the green dashed line. The purple box shows the magnitude of the observed event in MSWX (left).*

Dataset	Dominican Republic 5-day rainfall		Trend with GMST	
	Magnitude (mm)	Return period (95% C.I.)	Probability Ratio	Change in magnitude (%)
MSWX	149.3	6.46 (3.39 - 18.0)	1.32 (0.30 to 4.76)	13.7 (-50.5 to 88.3)
CHIRPS	96.0	6	0.37 (0.06 to 1.55)	-29.4 (-59.7 to 17.1)

Table 2.4: *Observed magnitude and estimated return period in current climate conditions for the 5-day rainfall associated with Melissa in MSWX, and the corresponding magnitude for a 6-year return period event in CHIRPS. Change in probability ratio and magnitude for Rx5Day in southern Dominican Republic with increasing GMST.*

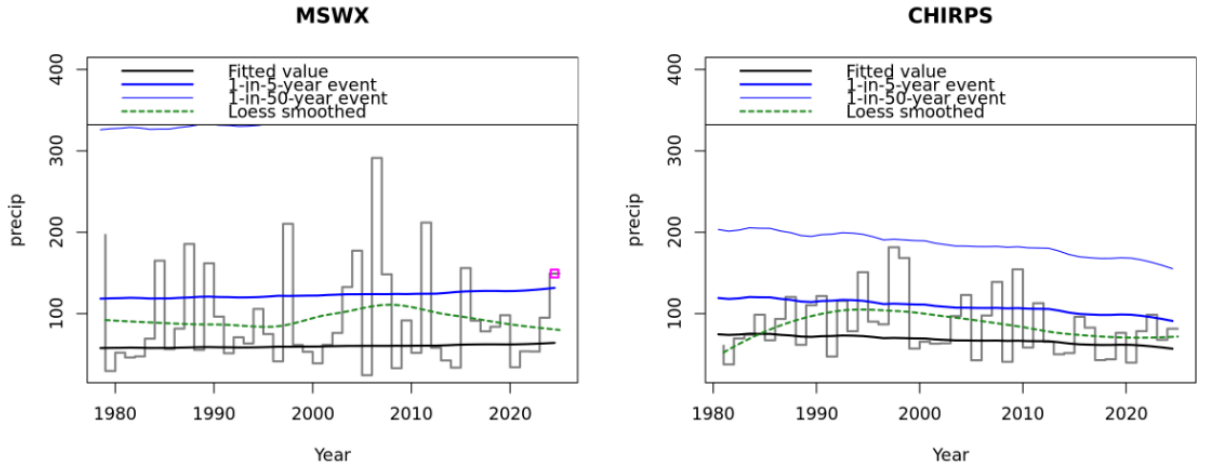

Figure 2.6: *Time series of September-November maxima of 5-day accumulated precipitation in the southern region of the Dominican Republic affected by Hurricane Melissa, in MSWX (left) and CHIRPS (right). The modelled influence of GMST on the expected value (5- and 50-year return period values) is shown with the black line (bold and lighter blue lines), while the loess smoothed trend is shown with the green dashed line. The purple box shows the magnitude of the observed event in MSWX (left).*

In the two regions affected by the heaviest rainfall, Jamaica and eastern Cuba, historical trends show a strong increase for the entire available record, since around 1980 (Figs. 2.1 - 2.4). The time-smoothed trend is captured well by the statistical model, giving strong increases in likelihood with warming relative to preindustrial climate conditions. In Jamaica, MSWX gives a statistically significant increase in likelihood by a factor of 3.5 (1.2 to 16) and in intensity by 64% (8 to 133%). CHIRPS shows a weaker factor increase of 1.5 (0.01 to 94) in likelihood and 11% (-56 to +76%) in intensity. Both estimates are above Clausius-Clapeyron scaling, and are consistent if the June-November period is considered, and for the 2-day accumulations (see appendices A.2.1 & A.2.2), though uncertainties are larger for the 2-day analysis.

In eastern Cuba, neither dataset gives results that are statistically significant at the 95% confidence level, but both suggest strong increases: MSWX gives an increase in likelihood by a factor of 9 (0.6 to inf) and in intensity by 55% (-23 to +125%), and CHIRPS gives an increase in likelihood by a factor of 7 (0.4 to 250) and in intensity by 53% (-15 to +184%). This is also significantly above Clausius-Clapeyron scaling and is consistent with the 2-day accumulations for the same region (see appendix A.2.2).

By contrast, in Haiti, the observed trends are small in magnitude and have high uncertainties (table 2.3), and in the Dominican Republic are different between the two datasets (table 2.4). This is partly due to a multi-decadal variability, visible in the smoothed trend (Figs. 2.5 & 2.6) that is not captured by the statistical model, as well as differences between datasets. It is worthy of note that Haiti and the Dominican Republic fall into a different Caribbean rainfall zone than Jamaica and eastern Cuba (Fig 3.1 in Climate Studies Group Mona 2020). Furthermore, the resultant trends are sensitive to the region studied, with different results and uncertainty levels for the wider nations or the subregions studied (see appendices A.2.2.3 & A.2.2.4). We conclude that additional data and validation of gridded datasets is required in these regions before any firm conclusions about the role of global warming on extreme rainfall like that due to Hurricane Melissa can be drawn.

2.2 Multi-method multi-model attribution

The climate model data used in this section are described in appendix A.1.2 and the model evaluation process is detailed in appendix A.3. The current section shows probability ratios and change in intensity for models that passed this model evaluation and also includes the values calculated from the fits with observations. These estimates are then synthesised into a final estimate of the attributable influence of GMST, and any other incorporated covariates, using the hazard synthesis procedure detailed in appendix A.4 and Otto et al. (2024). The synthesised results are also tabulated in Section 5 alongside the other hazard sections for ease of comparison, and the synthesis figures showing each model separately are shown in Section A.4.

2.2.1 Jamaica

Data		Rx5day	
		Probability ratio (95% CI)	**Intensity change (%) (95% CI)**
Observations	**Past- Present**	2.14 (0.097 to 43.9)	32.3 (-42.8 to 149)
Models		0.961 (0.341 to 3.32)	-0.0966 (-27.0 to 37.5)
Synthesis (Unweighted)		1.43 (0.143 to 14.4)	15.0 (-39.0 to 89.6)
Synthesis (Weighted)		1.06 (0.248 to 5.09)	4.39 (-32.7 to 53.4)
Weighted Model-Only Synthesis	**Present- Future**	1.03 (0.567 to 1.86)	2.19 (-16.7 to 20.9)

Table 2.5: *Synthesised probability ratio and change in intensity for 40-year return period for the September-November maximum 5-day rainfall period in Jamaica for observational datasets and the models that passed the evaluation tests, from pre-industrial climate to the present and from the present to 2.6℃ above pre-industrial climate. Trends close to 'no change' (change in intensity <5%) are highlighted in grey.*

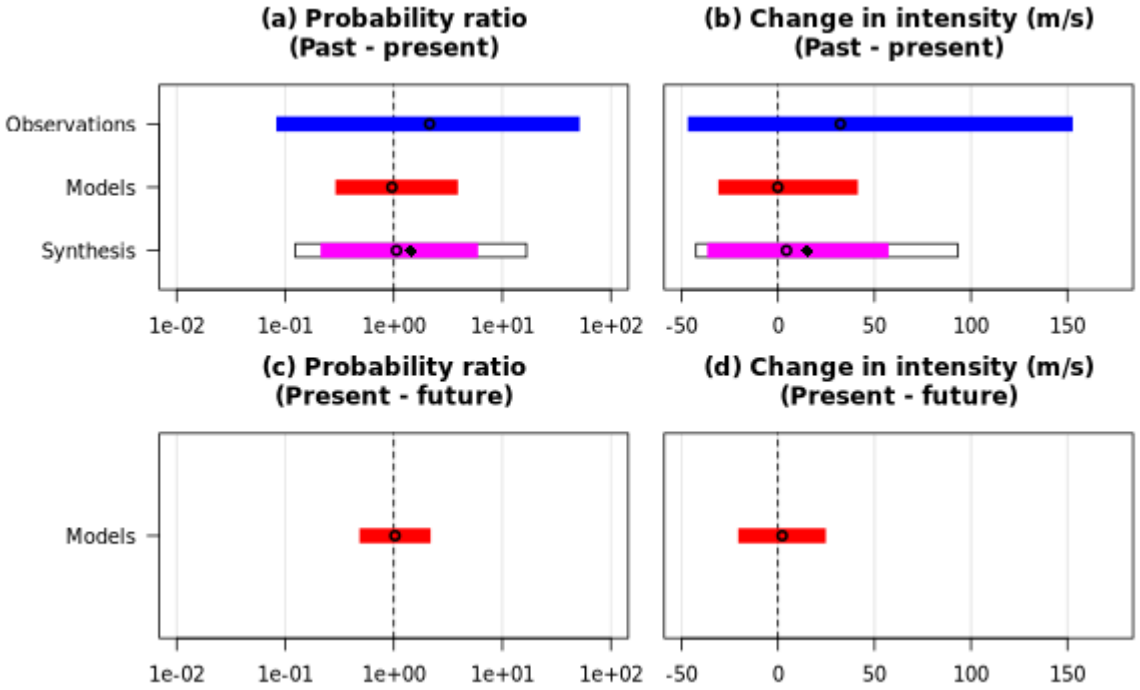

Figure 2.7: *Synthesised changes in (left) likelihood and (right) changes in intensity of Rx5Day in Jamaica when comparing (top row) the 2025 climate and a 1.3°C cooler climate representing the preindustrial past and (bottom row) the 2025 climate and a 1.3°C warmer climate representing the*

end of the century under current policies. Black diamonds indicate the unweighted mean of the observations and models.

2.2.2 Eastern Cuba

Data	Rx5day		
		Probability ratio (95% CI)	**Intensity change (%) (95% CI)**
Observations	**Past- Present**	8.91 (0.474 to 4650)	54.8 (-19.8 to 160)
Models		0.915 (0.431 to 2.56)	-1.94 (-25.3 to 29.4)
Synthesis (Unweighted)		2.85 (0.335 to 253)	23.2 (-25.5 to 86.8)
Synthesis (Weighted)		0.993 (0.393 to 4.74)	6.38 (-26.6 to 48.5)
Weighted Model-Only Synthesis	**Present- Future**	1.05 (0.656 to 1.67)	2.64 (-13.5 to 17.7)

Table 2.6: *Synthesised probability ratio and change in intensity for 10-year return period for the September-November maximum 5-day rainfall period in Cuba for observational datasets and the models that passed the evaluation tests. (a) from pre-industrial climate to the present and (b) from the present to 2.6℃ above pre-industrial climate. Trends close to 'no change' (change in intensity <5%) are highlighted in grey.*

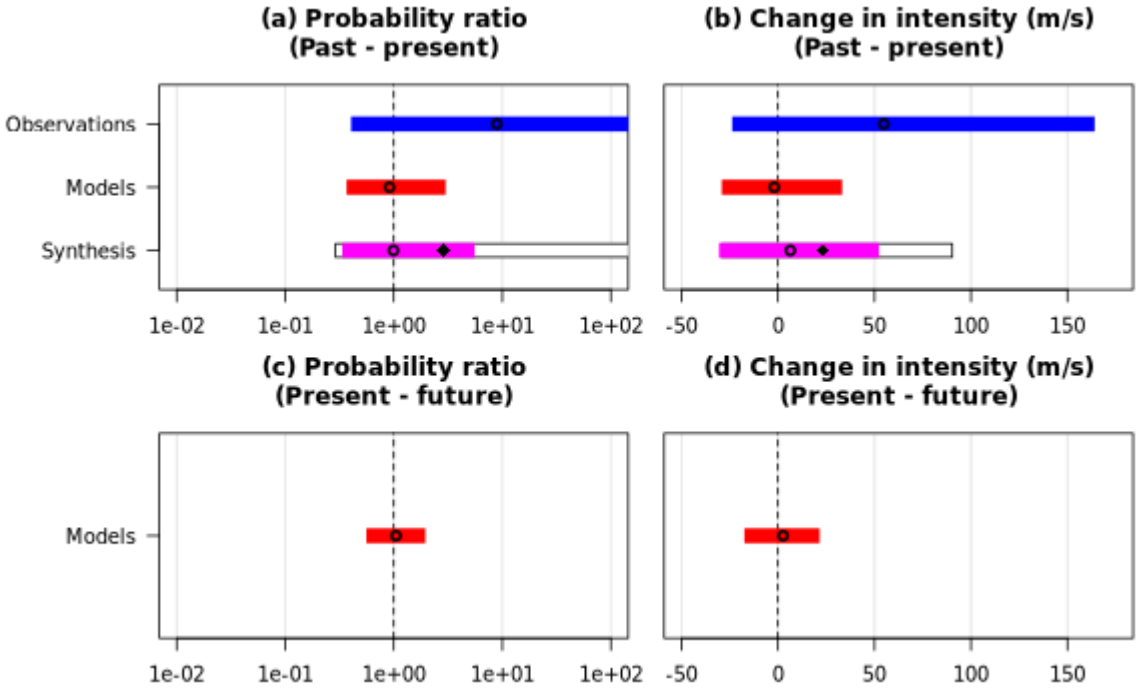

Figure 2.8: *Synthesised changes in (left) likelihood and (right) changes in intensity of Rx5Day in eastern Cuba when comparing (top row) the 2025 climate and a 1.3°C cooler climate representing the preindustrial past and (bottom row) the 2025 climate and a 1.3°C warmer climate representing the end of the century under current policies. Black diamonds indicate the unweighted mean of the observations and models.*

3 Potential Intensity attribution using WWA protocol

The event definition studied in this section is as follows:

1. ***Peak potential intensity (PI) in the Caribbean:*** *annual maxima of monthly potential intensity averaged over the sea surface from 80-60°W, 12-18°N (figure 1.3)*

In this section we use probabilistic attribution to examine the effect of climate change on peak monthly potential intensity in the Caribbean. We follow the World Weather Attribution protocol (Philip et al., 2020), using a nonstationary model in which the potential intensity is assumed to increase linearly with both GMST and the AMV. The data and statistical modelling used in this section are described in detail in appendix A.1.

The AMV is defined here as the decadally-smoothed detrended mean of the SSTs in the North Atlantic (0°-60°N, 0°-80°W), a region that encompasses the study region. The AMV has been linked to hurricane occurrence through its associations with Tropical North Atlantic wind shear (Knight et al., 2006) and its derivation from SSTs, which are highly correlated with potential hurricane intensity. Whilst the AMV is disputed as an internal mode of climate variability (Wei and Lohmann, 2012; Watanabe and Tatebe, 2019; Mann et al., 2021) significant multidecadal variability in Atlantic SSTs are clear in the past century (NOAA, 2025) and the fossil record (Knudsen et al., 2011). Independent of whether this phenomena is externally forced, there is a strong argument that similar multidecadal variability will continue to be observed in the near future, and therefore that its contribution to likely hurricane intensity should be considered.

Because the AMV is decadally smoothed and 2025 is the last year for which observed SSTs are currently available, we are unable to accurately estimate the 'true' 2025 value of the smoothed time series, and so can't quantify the contribution of the current AMV state to the high PI observed in October 2025. However, the addition of the AMV to the model improves the fit of the statistical model to the data by capturing the very low-frequency variability in the SSTs (the AMO alone accounts for about 43% of the variance of the annual PI time series), allowing us to isolate the warming trend and so reducing uncertainty about its strength. We therefore include the AMV in the statistical model for both observations and climate models, but don't quantify the contribution of the AMV to the intensity or likelihood of the 2025 potential intensity.

3.1 Observational analysis

Figure 3.1a shows the annual maxima of the monthly PI (calculated from monthly-resolution temperatures, humidity, pressure and sea surface temperatures from ERA5) over the study region. The black line shows the mean of a nonstationary normal distribution in which the mean shifts linearly with both GMST and the AMV, as described in Section A.1.3.1. The green dashed line is a nonparametric Loess smoother showing the empirical trend in the data over time; the fitted model tracks the nonparametric smoothed line closely, indicating that the chosen statistical model captures the large-scale trends in the data well.

Figure 3.1b shows the annual maxima of monthly PI as a function of the 4-year smoothed GMST (expressed as a difference from the 2025 observed GMST); here, there is a slight dip in the nonparametrically smoothed line at values of -1°C, but otherwise the fitted model captures the trend well. There is a clear increase in peak monthly PI as GMST increases, with peak PI now an estimated 3.7 m/s (95% bootstrapped confidence interval: 1.4 - 5.8 m/s) higher than it would have been without 1.3°C of human-caused warming.

Figure 3.1c shows the modelled change in return levels associated with a 1.3°C increase in GMST from the preindustrial to the current climate, with the AMV state kept fixed at the 2025 level. The points representing the potential intensities actually recorded in ERA5 lie very close to the lines representing the expected values, again indicating that the chosen statistical model represents the distribution of the data well. In the current climate, and in the 2025 AMV state, potential intensity as extreme as was observed in 2025 is estimated to be a relatively common event, with a return period of around 4 years.
There is a clear separation between the return levels in the current climate (red) and the past climate (blue); PI of the magnitude observed in October 2025 is estimated to be around 23 (4 - 200) times more likely, suggesting that in a climate without human-caused warming, similarly intense conditions would be expected to occur once every 100 years on average (16 - 800 years).

These results, along with the estimated return periods and changes in intensity for all datasets, are summarised in Table 3.1.

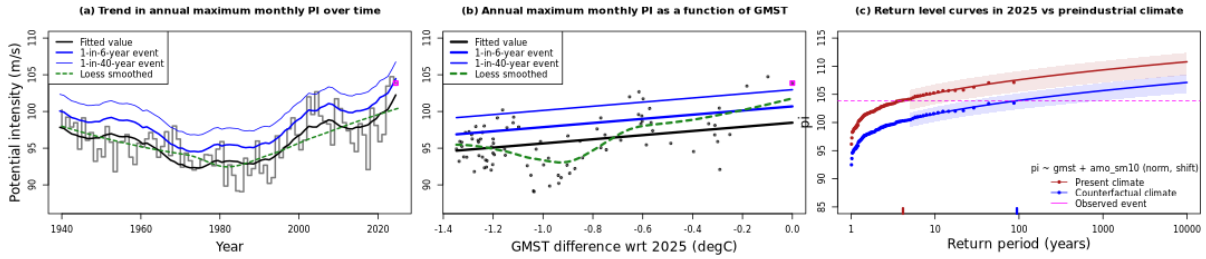

Figure 3.1: *Time series and fitted return levels of peak monthly potential intensity over the Caribbean. Data from ERA5.*

- *(a) Time series of peak monthly PI over the Caribbean, with fitted model overlaid. The pink dot marks the 2025 event; the heavy black line indicates the mean of the fitted model, and the blue lines indicate the expected return levels of 6- and 40-year events. The green line is a nonparametric Loess smoother.*
- *(b) Linear trend in peak monthly PI over the Caribbean as a function of GMST (shown as a difference from the 2025 GMST). The pink dot marks the 2025 event; the thick black line denotes the nonstationary location of the fitted distribution, and the blue lines show estimated 6- and 40-year return levels. The 2025 observation is highlighted in magenta.*
- *(c) Expected return levels of peak monthly PI over the Caribbean in the 2025 climate (red line) and in a 1.3°C cooler counterfactual climate (blue line), estimated using the statistical model described in section A.1.3.1. Shaded regions represent 95% confidence intervals obtained via a bootstrapping procedure. The pink line shows the PI observed during October 2025. Red and blue ticks at the x axis indicate the estimated return level of the event in the 2025 climate and 1.3°C cooler climate.*

	Event magnitude	Return period	Probability Ratio	Change in

Dataset	(m/s)			magnitude (m/s)
ERA5	103.9	4.2 (1.9 - 17.6)	**22.7** **(3.9 - 204)**	**3.67** **(1.50 - 5.70)**

Table 3.1: *Return period, change in probability ratio and magnitude for the potential intensity in October 2025 in a region around the track of Hurricane Melissa, due to GMST.* ***Bold*** *text shows statistical significance at the 95% confidence level.*

3.2 Multi-method multi-model attribution

This section shows Probability Ratios and change in intensity ΔI for models that passed model evaluation and also includes the values calculated from the fits with observations. The synthesis procedure used to produce Figure 3.2 is described in appendix A.4 (see Otto et al., 2024). The synthesised results are also tabulated in section 6 alongside the other hazard sections for ease of comparison, and the synthesis figures showing each model separately are shown in Section A.4.

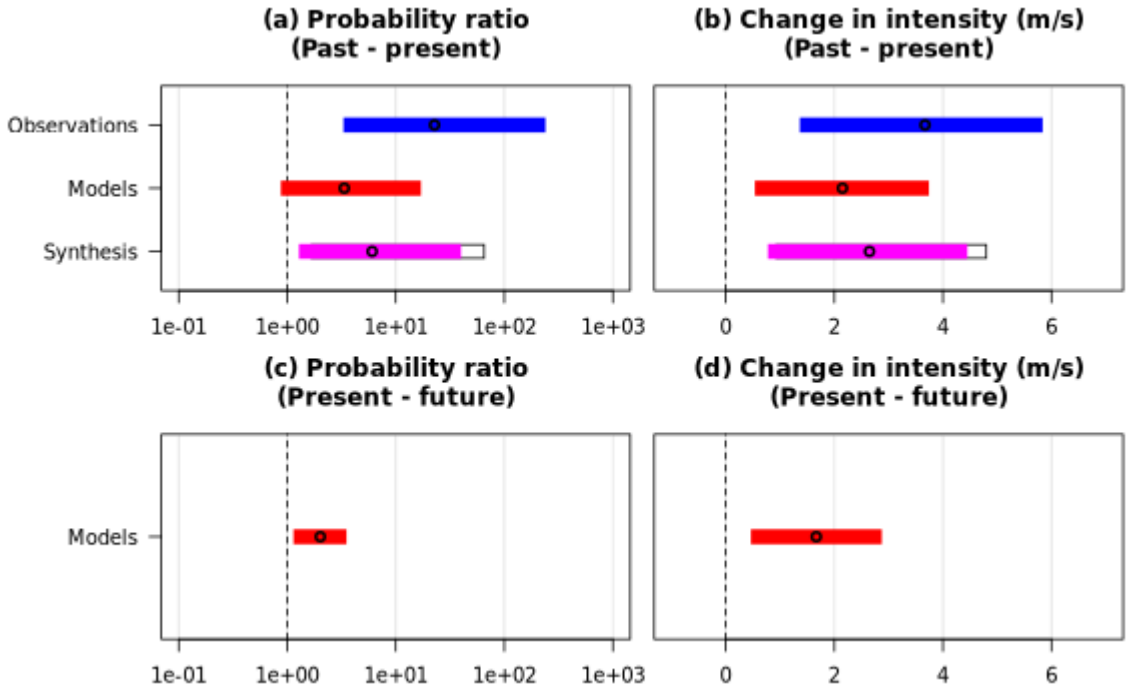

Figure 3.2: *Synthesised changes in (left) likelihood and (right) changes in intensity of similarly extreme potential intensity in the Caribbean when comparing (top row) the 2025 climate and a 1.3°C cooler climate representing the preindustrial past and (bottom row) the 2025 climate and a 1.3°C warmer climate representing the end of the century under current policies.*

Data source	**Period**	**Probability ratio**	**Change in intensity (m/s)**
ERA5	Past - Present	**23**	**3.67**

		(3.9 to 204)	**(1.50 to 5.70)**
Models		**3.4 (1.02 to 15)**	**2.15 (0.67 to 3.60)**
Synthesis (unweighted)		**8.7 (1.9 to 56)**	**2.91 (1.06 to 4.67)**
Synthesis (weighted)		**6.1 (1.5 to 34)**	**2.65 (0.91 to 4.31)**
Models	Present - Future	**2.02 (1.34 to 3.00)**	**1.67 (0.60 to 2.73)**

Table 3.2: *Summary of synthesised changes in (a) probability ratio and (b) change in intensity of peak monthly PI over the Caribbean with a return period of 5 years in the current climate, also visualised in Figure 3.2. 95% confidence intervals are given in brackets. Statistically significant changes are highlighted in* ***bold****.*

4 Wind speed and extreme rainfall attribution using IRIS

The event definitions studied in this section are as follows:

1. **Jamaica rainfall:** eyewall rainfall rate from hurricanes making landfall on Jamaica
2. **Jamaica landfall:** wind speeds of hurricanes making landfall on Jamaica with a maximum sustained wind speed of at least 80 m/s immediately prior to landfall (figure 1.4)

Assessing tropical cyclone risk given the infrequency of landfalling tropical cyclones and the short period of reliable observations remains a challenge. Synthetic tropical cyclone datasets can help overcome these problems. We explore this method here using a global tropical cyclone wind model (IRIS) with several key innovations. It recognises that the key step for estimating landfall wind speed is the location and value of the life-time maximum intensity (LMI), where the cyclone reaches its highest wind speed. It redefines the problem as one of decay only. The initial intensity, life-time maximum, is assumed to be physically constrained by the thermodynamic state as defined by the potential intensity (PI).

4.1 Attribution of rainfall

The change in eyewall rain rate (maximum azimuthal mean rain rate) for an event like Melissa striking Jamaica is clear. Such events now occur roughly once every 39 years, but prior to warming of 1.3°C would have occurred only once every 56 years (Figure 4.1). This represents an increase in likelihood of approximately 43%. Equivalently, events of a similar rarity to Melissa in preindustrial times would have been approximately 2.1 mm/hr lighter (0.6 mm/hr heavier to 5.2 mm/hr lighter). This is an increase of 15.6% (-4.5% to +38.8%). This result is also in line with the change in rainfall over the Jamaica region shown in section 2.2.1 (and summarised in section 5), in which the unweighted synthesis of observations and climate models gave a change of +15% (-39 to +90%), and observations alone suggest a larger increase.

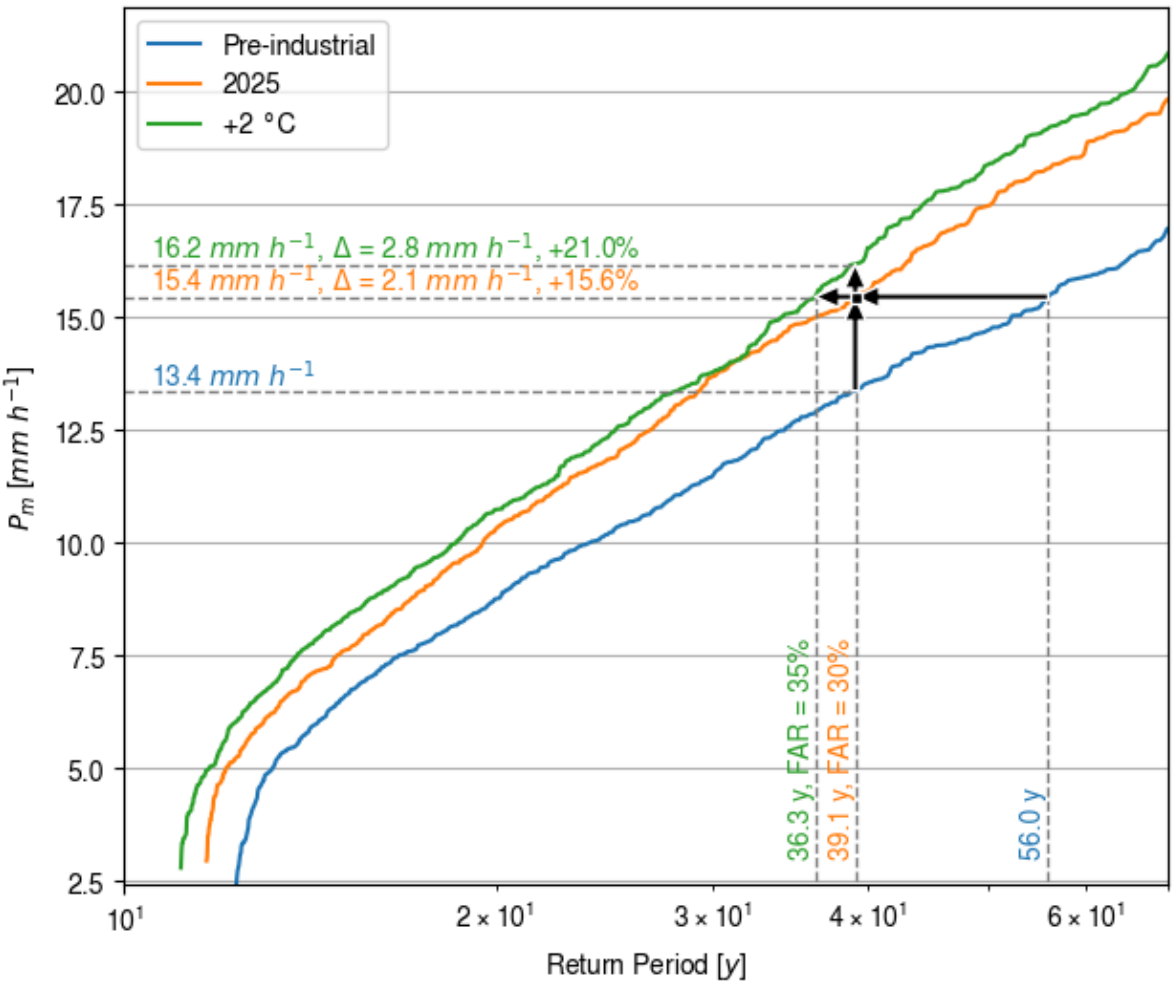

Figure 4.1: *Maximum azimuthal mean rain rate for hurricane landfall in Jamaica vs return period as calculated for the current climate "2025" (+1.3°C, orange line), pre-industrial (blue line) and +2°C climate (green line). FAR is the Fractional Attributable Risk (Equation 1) of landfall with a maximum azimuthal mean rain rate of 15.4 mm/hr (obtained from IMERG) in the current climate. Δ shows the increase in rain rate compared to pre-industrial "Melissa" type events.*

4.2 Attribution of wind speeds

The change in return period of the landfall wind speed for an event like Melissa striking Jamaica is clear. Such events remain extremely rare, but now occur roughly once every 1700 years, whereas prior to warming of 1.3℃ would have occurred only once every 8100 years. This represents an increase in likelihood of approximately a factor of 4.8 (2.6 to 9.6). Equivalently, events of a similar rarity to Melissa in preindustrial times would have been approximately 5.1 (2.3 to 8.1) m/s slower. This result is also in line with the attributed change in PI over the Melissa track shown in section 3.2 and summarised in section 5, which gave a change in likelihood of a factor of 6 (1.5 - 34), and a change in intensity of +2.6 (0.9 - 4.3) m/s.

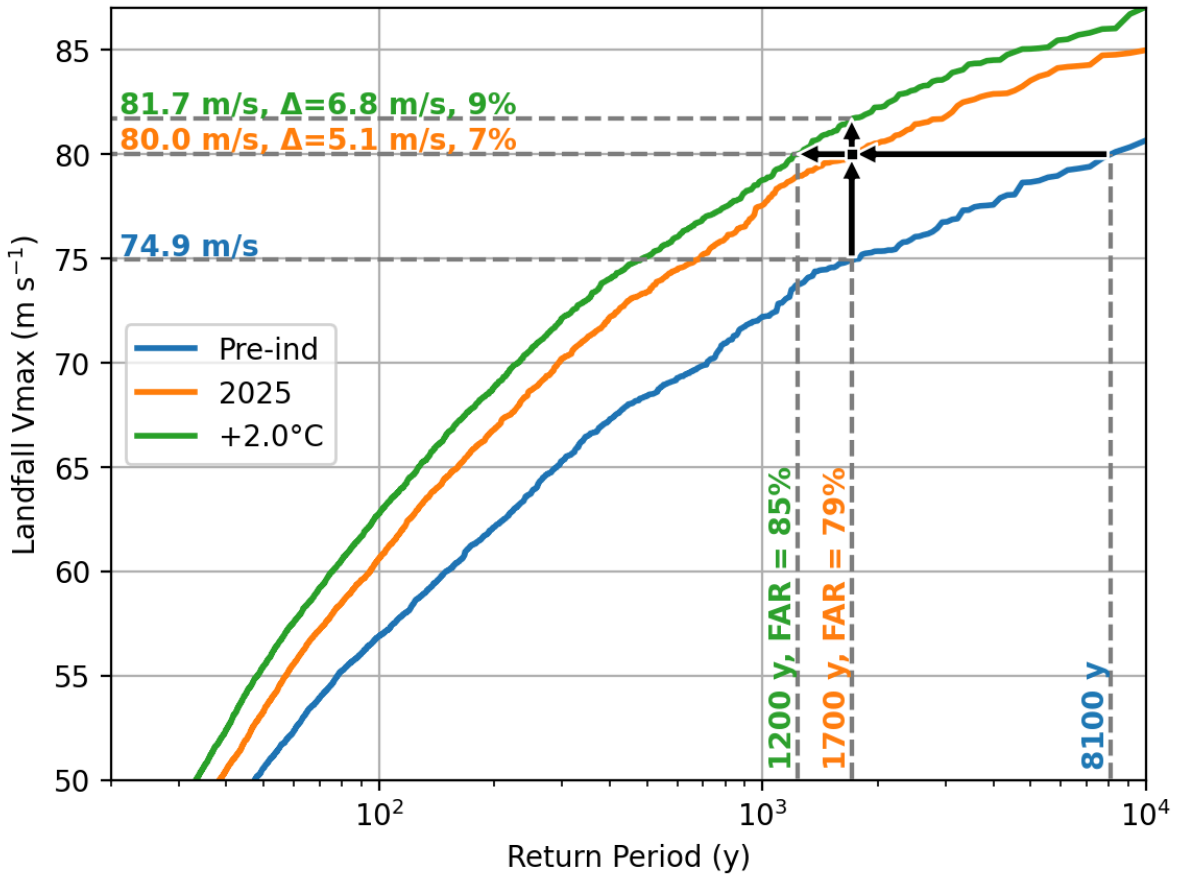

Figure 4.2: *Return curves for maximum wind speeds in tropical cyclones making landfall in Jamaica. The orange curve shows the present day climate in 2025, the blue curve shows the pre-industrial climate, green shows the +2°C climate.*

4.3 Interpretation of results

This is a new approach, used in three rapid studies to date (Clarke et al., 2024a; Clarke et al., 2024b; Clarke et al., 2024c), that sits alongside the usual WWA protocol. First, it is a single model, whereas WWA normally combines multiple models and approaches into a single statement. In general, additional models help to sample a wider range of possibilities to ensure that we are as close to reality as possible. However, this approach is fundamentally different in nature. It is a stochastic model that is not based on climate models, only on observations and well understood physics. This means that it is not subject to the same biases and challenges around simulating phenomena at small scales that climate models struggle with. Furthermore, it is based on a very large number of data points (~100000 years of synthetic data) and the results are tested against observed storm tracks and intensities.

With its basis in fairly simple and robust thermodynamic and physical arguments, this method is complementary to the WWA protocol. In particular, for tropical cyclones, it allows us to make statements about wind speeds that we cannot do on a rapid basis using the traditional method. This is because climate models (and therefore our method) are fundamentally limited in their ability to resolve the phenomena leading to these intensities. This approach just leverages other knowledge to bypass that challenge. However, overall, the results are still valid for the 'class of event' in the same

way as our normal results, and thus the interpretation is essentially the same. Similarly, as shown by the study of storms close to the point of landfall, the analysis can be constrained in various ways so that they are as close to the impacts as we can manage.

5 Hazard summary

This section contains all of the final results for each hazard analysis, including the probabilistic event attribution of extreme rainfall and potential intensity, using the WWA method, and the IRIS analysis of extreme rainfall rate and wind speeds.

The return period of the 5-day accumulated rainfall from Melissa in Jamaica is about 40 years, and in eastern Cuba about 10 years, based on the gridded dataset MSWX. We highlight that the results are from a single gridded dataset available in near real time and are therefore likely an underestimate of total rainfall. Notably, the return period of the extreme rainfall rate in IRIS was also around 40 years, though this represents an hourly rate rather than multi-day accumulation. Observations and models disagreed whether climate change from the preindustrial period to present has driven increases in likelihood and intensity of similar 5-day extremes across both regions, with consistent increases in observations and mixed trends in models (table 5.1). The difference between the observed and modelled trends is likely due in part to the resolution of the models. While the highest resolution models used (~25km) are broadly able to resolve small islands and key elements of tropical cyclone structure, they may still fail to capture the most intense rainfall totals owing to interactions between complex topography and cyclones. Further research and modelling capacity is urgently needed in this highly exposed and understudied region.

The discrepancy in observed and modelled trends leads to a synthesised result for models very close to no change in both regions, as well as a weighted synthesis close to no change (table 5.1), see Otto et al. 2024 for details on the weighting and synthesis method. When assessing whether there is a trend in likelihood and intensity in the future at 2.6°C of warming the models also project essentially no change for events like Melissa. Given the broad disagreement between observed and modelled trends, and the known deficiencies of the models we also communicate the unweighted synthesis. In this case, the unweighted synthesis places relatively larger weighting on the observations, which have higher uncertainty ranges, and results in increasing trends in both regions. In Jamaica, the likelihood of an event like Melissa has increased by a factor of 1.4 (0.14 to 14) and in intensity by 15% (-39 to 90%) (approximately 1.6x Clausius-Clapeyron scaling). In eastern Cuba, the likelihood of an event like Melissa has increased by a factor of 2.9 (0.34 to 250) and in intensity by 23% (-26 to 87%) (approximately 2.5x Clausius-Clapeyron scaling).

In order to determine a final attribution statement for the changes in heavy rainfall associated with hurricanes like Melissa, several lines of evidence are taken into account beyond the observed and modelled trends described above. First, the underlying thermodynamic argument suggests that a warmer atmosphere will tend to hold more moisture at a rate of 7% per °C, suggesting an a priori expected increase of approximately 9%. Second, the other rainfall analysis in this report, analyzing the eyewall rainfall rate using the IRIS system, shows that the eyewall rain rate experienced in Jamaica due to Melissa has also increased due to warming, becoming approximately 43% more likely (from a 56 year event down to a 39 year event) and about 2 mm/hr (-0.6 to +5.2 mm/hr) or 16% (-4.5 to +39%) more intense. Though this method focuses on tropical cyclones specifically, contrary to the WWA method, it is striking in agreement with the unweighted synthesis for Jamaica. Third, several other attribution studies for hurricanes in the region exist (see section 1.1), and across those studies all point towards enhanced hurricane rainfall in the wider region.

Combining these lines of evidence including the strength of observed trends, known model deficiencies, physical reasoning, the IRIS analysis, and many other attribution studies for the region using a range of methods, we conclude that climate change has amplified the amount of rainfall in

both regions. While it is difficult currently to quantify the change in likelihood of such an event, the consistency in the results of two different analyses in this report as well as across other attribution studies suggests that the rainfall intensity change exceeds Clausius-Clapeyron scaling (>9% at 1.3°C warming).

Data		Jamaica 5-day rainfall		Eastern Cuba 5-day rainfall	
		Probability ratio (95% CI)	**Intensity change (%) (95% CI)**	**Probability ratio (95% CI)**	**Intensity change (%) (95% CI)**
Observations	**Past-Present**	2.14 (0.097 to 43.9)	32.3 (-42.8 to 149)	8.91 (0.474 to 4650)	54.8 (-19.8 to 160)
Models		0.961 (0.341 to 3.32)	-0.0966 (-27.0 to 37.5)	0.915 (0.431 to 2.56)	-1.94 (-25.3 to 29.4)
Synthesis (Unweighted)		1.43 (0.143 to 14.4)	15.0 (-39.0 to 89.6)	2.85 (0.335 to 253)	23.2 (-25.5 to 86.8)
Synthesis (Weighted)		1.06 (0.248 to 5.09)	4.39 (-32.7 to 53.4)	0.993 (0.393 to 4.74)	6.38 (-26.6 to 48.5)
Models only	**Present-Future**	1.03 (0.567 to 1.86)	2.19 (-16.7 to 20.9)	1.05 (0.656 to 1.67)	2.64 (-13.5 to 17.7)

Table 5.1: *Summary of results for 5-day September-November rainfall maxima in Jamaica and eastern Cuba, presented in Figs 2.7&2.8: changes due to GMST include past-present changes and present-future changes. Trends very close to 'no change' (change in intensity <5% and/or change in PR < 0.1) are highlighted in grey.*

Changes in the potential intensity conditions forming such a storm are shown in table 5.2. Models and observations strongly agree on increases due to GMST, though observations give a much stronger trend to date. Synthesising both data sources, we find that such conditions have become significantly more likely at around a factor of 6.1 (1.5 to 34) and with a change in intensity of 2.7 (0.9 to 4.3) m/s. In future, models project a further doubling (1.3 to 3) in the likelihood of such conditions.

Data		Potential intensity	
		Probability ratio	**Change in intensity (m/s)**
Observations	**Past - present**	**22.7 (3.9 to 204)**	**3.67 (1.50 to 5.70)**
Models		**3.35 (1.02 to 14.5)**	**2.15 (0.67 to 3.60)**
Synthesis		**6.06 (1.50 to 34.0)**	**2.65 (0.91 to 4.31)**
Models only	**Present - future**	**2.02 (1.34 to 3.00)**	**1.67 (0.60 to 2.73)**

Table 5.2: *Summary of results for annual maximum of monthly PI over the study region, presented in Fig 3.2: changes due to GMST include past-present changes and present-future changes. Statistically significant changes are highlighted with* ***bold text****.*

Finally, using IRIS, the wind speed of storms like Melissa making landfall in Jamaica have increased due to warming, becoming approximately 5 times more likely (from an 8100 year event down to a 1700 year event) and about 5 m/s (2.3 to 8.1 m/s) more intense (table 5.3). Similarly, as described above, the eyewall rain rate experienced by Jamaica due to Melissa has also increased due to warming, becoming approximately 43% more likely (from a 56 year event down to a 39 year event) and about 2 mm/hr (-0.6 to +5.2 mm/hr) more intense. Both of these changes are expected to increase further at 2°C of warming.

Variable	**Preindustrial - present (1.3°C)**		**Preindustrial - future (2°C)**	
	Probability ratio	**Change in magnitude**	**Probability ratio**	**Change in magnitude**
Eyewall rain rate	1.43 (0.90 to 2.36)	+2.1 mm/hr (-0.6 to +5.2 mm/hr) +15.6% (-4.5 to + 38.8%)	**1.54** **(1.02 to 2.56)**	+2.8 mm/hr (-0.4 to +6.0 mm/hr) +21% (-3.0 to +44.8%)
Wind speeds	**4.8** **(2.6 to 9.6)**	**+5.1 m/s** **(+2.3 to 8.1 m/s)** **+6.8%** **(+3.1 to 10.8%)**	**6.8** **(3.7 to 12.4)**	**+6.8 m/s** **(+3.9 to +9.3 m/s)** **+9.1%** **(+5.2 to 12.4%)**

Table 5.3: *Summary of results for eyewall rainfall rate and wind speeds, presented in Figs. 4.1 & 4.2: changes due to GMST include past-present changes and past-future changes of 2°C.* ***Bold text*** *shows statistical significance at the 95% confidence level.*

6 Vulnerability and exposure

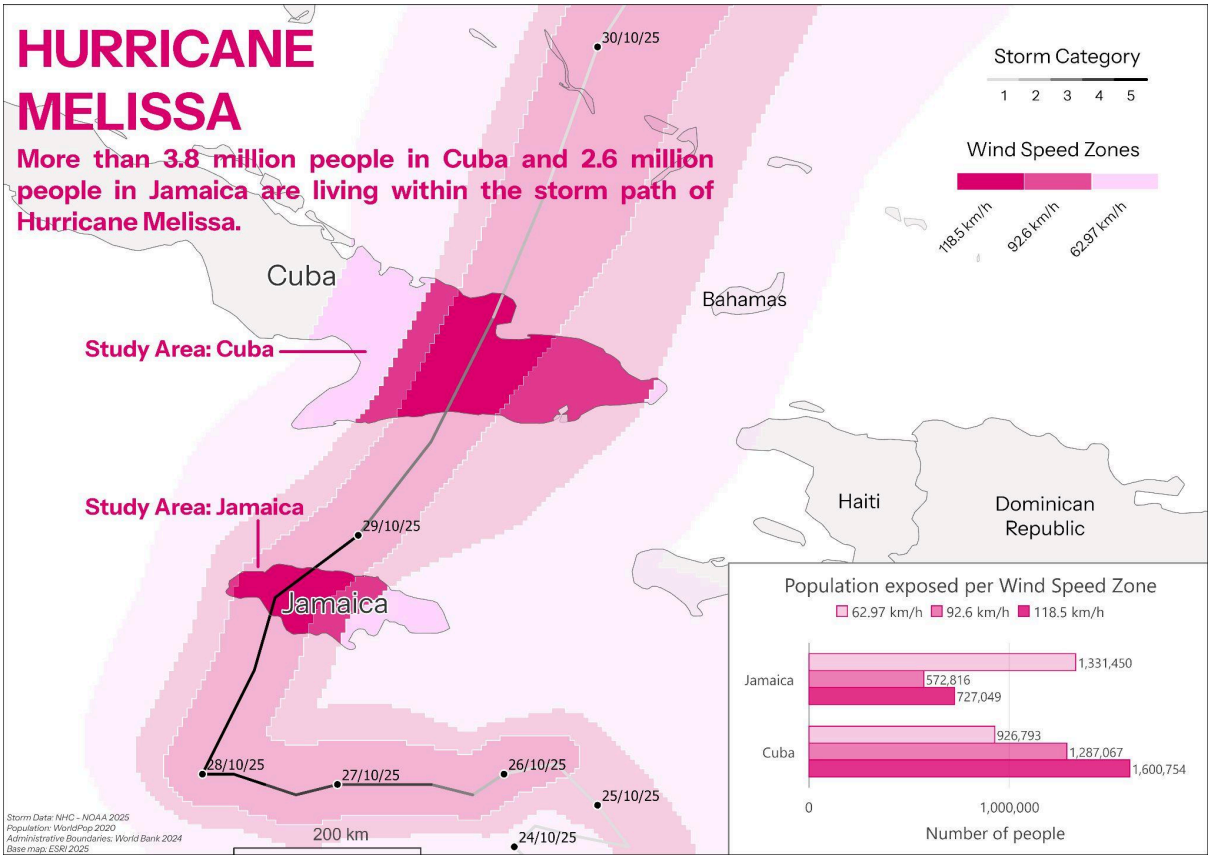

Figure 6.1: *Population exposure per wind speed zone of Hurricane Melissa. Data: Storm Data: NHC - NOAA 2025; Population: WorldPop 2020; Administrative Boundaries: World Bank 2024; Base map: ESRI 2025.*

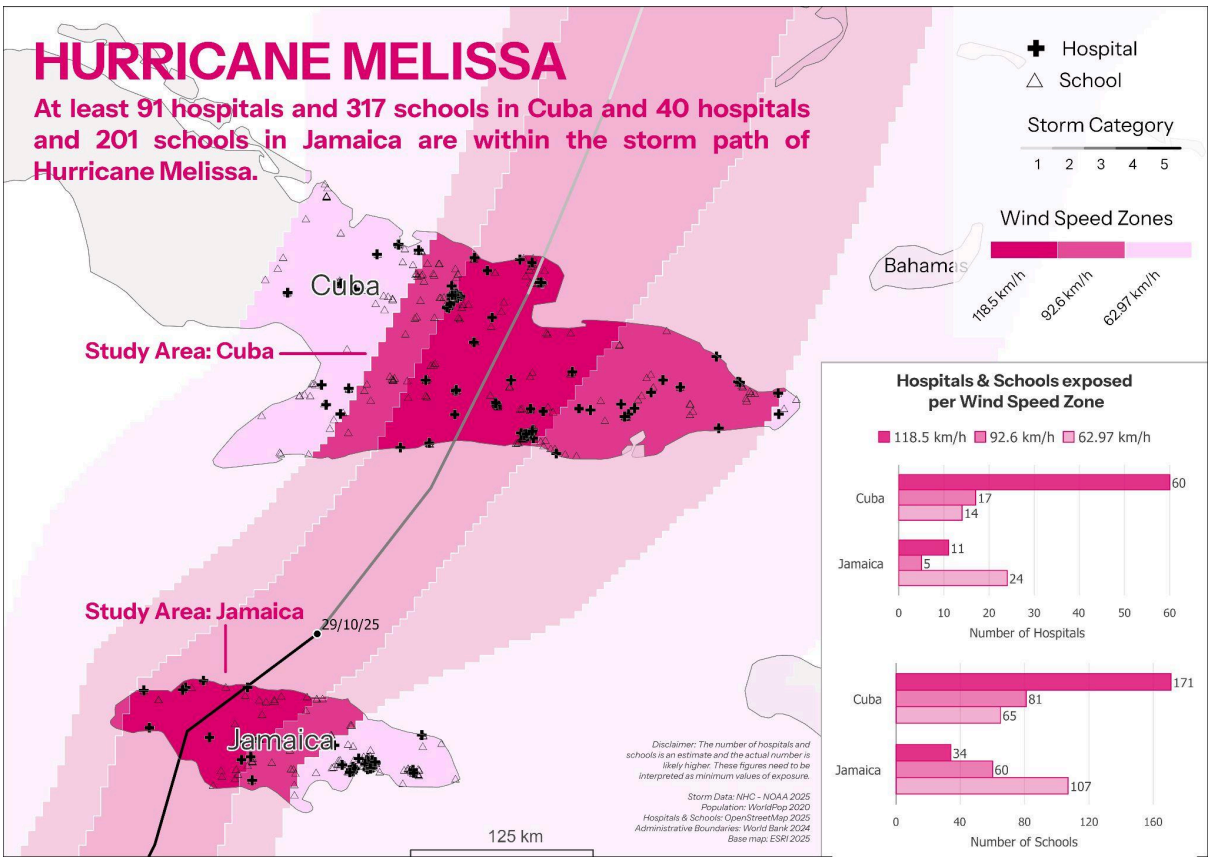

Figure 6.2: *Population exposure per wind speed zone of Hurricane Melissa. Data: Storm Data: NHC - NOAA 2025; Population: WorldPop 2020; Hospitals & Schools: OpenStreetMap 2025; Administrative Boundaries: World Bank 2024; Base map: ESRI 2025. Disclaimer for Schools & Hospitals: The number of hospitals and schools were derived from OpenStreetMap and are an estimate. The actual number of exposed infrastructure is likely higher. These figures need to be interpreted as minimum values of exposure.*

The impacts from Hurricane Melissa are not a result of only the physical hazard, but also the exposure of people and assets to that hazard, and their vulnerability, the propensity for those people and assets to be impacted. Therefore, this section is a rapid analysis of vulnerability and exposure factors that both may have contributed to impacts, or helped avoid them. We primarily focus on Jamaica, due to the unprecedented nature of the storm there, with a secondary focus on Cuba and Haiti given the subsequent landfall and high death tolls there, respectively. Given this is a rapid analysis, the full extent of the impacts of the storm are likely to only become clear in the weeks that follow once emergency response teams can reach and survey areas that are currently unreachable and communications networks have been restored. At the time of writing, there have been at least 32 deaths reported in Jamaica, 30 in Haiti, 4 in the Dominican Republic, 3 in Panama (Jamaica Gleaner, 2025; BBC, 2025A; BBC, 2025B). Forty hospitals in Jamaica and 90 in Cuba were exposed to extreme winds, as well as 201 schools in Jamaica and 317 in Cuba, representing just some of the critical infrastructure exposed to damaging winds (Figure 6.2). In Jamaica, of the thousands of persons displaced, approximately 25,000 relocated to emergency shelters (JIS, 2025). Preliminary satellite assessments of infrastructure damage indicate widespread damage to structures (homes, buildings, roads, bridges), including 1,107 buildings 100% damaged in Crawford Village, Saint Elizabeth Parish near the landfall site in Jamaica (UNOSAT, 2025; PDC, 2025). At least 3 major

hospitals were severely impacted by the storm, prompting emergency evacuations of patients and staff (PAHO, 2025). Notably the particularly high death toll in Haiti has been linked to riverine flooding in Petit-Goave in news reports (USA Today, 2025).

Important to note is that Jamaica was still recovering from Hurricane Beryl, which tracked along the island's southern coast just 16 months earlier, on July 3, 2024 in a similar part of the island (IFRC, 2025; Reuter, 2025). At least four fatalities were reported, most of them related to flooding. Beryl caused an estimated $6.5 billion in damage, dropping Jamaica's GDP by 1.9% compared to 2023 (UN, 2024). Rural areas of Jamaica were hit particularly hard, causing major losses to agriculture (UN, 2024). Physical infrastructure, such as Munro College in St. Elizabeth, which was badly affected by Beryl, was said to have recovered well and to be adequately prepared for Melissa (The Gleaner, 2025). However, a hospital in the same parish had to move patients on higher floors as the building was still damaged from hurricane Beryl (BBC, 2025a). Collective memory of the past disaster seemed to help Jamaicans to prepare for hurricane Melissa, though people in the country have no prior experience with an event of this magnitude (see Local10.com, 2025; The Gleaner, 2025; The Guardian, 2025), however, the close proximity of the two storms was reported to take a mental toll on the population (see ABC news, 2025; PBS, 2025). Coastal communities remained especially financially vulnerable after Beryl and livelihoods have not been fully restored (UN, 2025a).

In disaster-prone small-island states like Jamaica there is a persistent challenge in balancing spending limited funds on disaster preparedness and recovery, reducing fiscal deficit, and advancing growth (Natural hazard risk reduction strategy, Jamaica, 2005). Funds spent on the former, reduce the budget for other areas such as education and healthcare, which in turn reduce the country's resilience to climate extremes.

7.1 Population vulnerability

In general, those with pre-existing health conditions, disabilities, especially limited mobility, lower income groups, and historically disadvantaged groups tend to be the most vulnerable during and after hurricanes (Ganz et al., 2023; Parks et al., 2023). This is for a variety of reasons such as having a lower ability to physically evacuate quickly, less awareness of emergency procedures or directives, lack of disposable income to evacuate, reliance on particular medical devices especially those that run on electricity, feeling unsafe in shelters, lack of social connections when essential services are down, and many others.

Jamaica

In its disaster risk management strategy, the Jamaican government has highlighted children, youth-at-risk, the elderly, persons with disabilities (PWDs), women, and persons and families living below the poverty line, persons living in some rural communities, coastal zones and low-lying areas, people with poor housing and the homeless as vulnerable (ODPEM, 2022).

The parish of St. Elizabeth, where Hurricane Melissa made landfall is 84% rural, with 10% of the population over 65 years, and 26% below 15 years. Disasters have impacts not only on the population but on almost all economic industries and sectors – tourism, agriculture, education, and health among others (ODPEM, 2022). The Office of Disaster Preparedness and Emergency Management (ODPEM)

has identified over 700 vulnerable communities nationwide. Many of these have a high incidence of substandard housing and are located in hazardous areas, such as floodplains and steep slopes (The Community Renewal Index (CRI)). Approximately, 82% of the population live within five kilometers of the coast and 70-90% of the economic, industrial and essential infrastructure in Jamaica is concentrated in vulnerable low-lying areas susceptible to storm surges, riverine flooding and flash-floods post high levels of precipitation. (Avenlon-Cullen, et al, 2023; WBG, 2025).

Cuba

Hurricane Melissa primarily impacted the southeastern provinces of Santiago de Cuba, Granma, Holguín, Guantánamo, and Las Tunas which includes a mix of urban centres and rural areas. Many of these areas are increasingly vulnerable to drought impacting food and water resources (UNDRR, 2024) For example, the province of Santiago de Cuba has heightened vulnerability in terms of food and nutrition security due to severe drought which has worsened since 2015 (SDGF, 2019, UNDP) Its capital, also called Santiago de Cuba, is also susceptible to impacts of hydro-meteorological events due to its geographical location and weakened infrastructure-it has a population of over half a million people of which 90 % live in high rise buildings with weakened sanitation and water storage provisions (SDGF, 2019). Cuba ranks high on the Human Development Index (HDI) with 0.762 in 2023 (UNDP). Due to lack of up-to-date data and research on Cuba, there are limitations to fully characterising population vulnerability.

Haiti

Despite not making landfall in the country, above average rainfall prior to Hurricane Melissa, which continued through the period, caused extensive flooding in the southern region which caused loss of life, infrastructure damage and destruction of crops and plantations. (FEWSNET, 2025) Over the past 30 years Haiti has experienced close to 100 storms, flooding and hurricane events while also being impacted by periodic droughts (World Bank, 2024, GFDRR, 2025). These high levels of extreme events over years have contributed to, for example, lower crop production and inadequate water provisioning, adversely contributing to malnutrition, water and vector-borne diseases and mental health impacts (World Bank, 2024). In addition, political instability, economic issues, and escalating violence has left the population highly vulnerable to shocks and stresses (World Bank, 2025; GFDRR, 2025). While climate hazards do not cause armed conflict, they can amplify existing inequality and tensions (ICRC, 2020, Sitati, 2021). There is currently a severe humanitarian crisis ongoing with widespread displacement, poverty, food insecurity, and lack of access to basic services (WFP, 2025). This high degree of vulnerability is likely, at least in part, driving the high death toll in Haiti from Hurricane Melissa.

7.2 Exposure and landuse

The spatial configuration of storm risk associated with Hurricane Melissa reflects a complex interplay between geophysical exposure, land use dynamics, and environmental management across the northern Caribbean. Jamaica's mountainous terrain and narrow coastal plains create distinct hazard risks: storm surges and coastal flooding threaten low-lying areas, while intense winds and landslides are concentrated in upland regions such as the Blue Mountains and the interior of its parishes (WFP, 2025). Cuba's largely low-lying agricultural and coastal zones also face exposure to storm surges and flooding, particularly in productive plains and coastal settlements (UNDP, 2024). In Haiti, storm risk

is similarly magnified across low-lying, densely populated plains, valleys, and mountainous regions where steep slopes, deforestation, and intense rainfall amplify landslide and flood risk. A dense river network further channels run-off through exposed communities (World Bank, 2024).

Jamaica

In Jamaica, more than half the island remains forested, and overall forest cover increased by 7.9% between 2013 and 2023 due to regrowth on abandoned agricultural lands (Forestry Department, 2024). Deforestation rates remain low (0.46% annually), with regeneration largely matching losses (Bowers et al., 2021). Nonetheless, hillside deforestation and the degradation of mangroves, coral reefs, and wetlands continue to elevate landslide and storm surge exposure. Mining in Long Bay has contributed to further soil extraction which has damaged the sea barrier (MacDougall, 2017). Agriculture remains a dual driver of change: large-scale holdings clear vegetation, while abandonment on smaller farms promotes secondary forest regrowth (Bowers et al., 2021).

Urbanization and infrastructure expansion - particularly roads, energy infrastructure, and coastal development - are major land-use drivers. For example, construction of Highway 2000 connecting Kingston and Ocho Rios, powerlines in Clarendon, and solar installations in Westmoreland have transformed peri-urban landscapes (Forestry Department, 2024; Bowers et al., 2021). Built-up area increased by 33.8% between 2013-2023 (Forestry Department, 2024), largely along coastal plains around Kingston, St Catherine, St James, Trelawny, and St Ann.

Informal settlements, though more dispersed, remain highly exposed to flooding and wind damage (Bowers et al., 2021). Over 20% of Jamaica's population live in informal/unregulated settlements (Government of Jamaica, 2014). Informal settlements have no formal planning approval and therefore rarely benefit from site development standards, building codes, and engineering standards, which serve to protect public health and safety. In 2023 the Disaster Vulnerability Reduction Project (DVRP) undertook, amongst others, to improve construction standards which varied significantly across municipalities. Building standards can help withstand earthquakes, hurricanes, floods, landslides, and heat. Jamaica has several planning authorities and regulatory agencies that enforce building codes, however some municipalities have limited technical practitioners to apply national building codes and disrupt or prevent the emergence of informal settlements.

Cuba

Cuba has undergone notable land-cover transformation over the past 35 years, marked by widespread reforestation and agricultural abandonment following economic shifts post the collapse of the Soviet Union in the 1990s (Machado, 2018). Forested and shrubland areas rose from 17% in 1985 to over 38% in 2020, while agricultural lands fell from about 60% to 41% (Nunez-Penichet, Maita & Soberon, 2024). Simultaneously, urban and peri-urban agriculture has emerged as an adaptive strategy for food security, including in Havana (McNamara, 2017). Yet recent declines in reforestation efforts (-40% in new plantings since 2020) and growing wildfire incidence signal emerging vulnerabilities (Global Forest Watch, 2025).

Haiti

In Haiti, forest loss has been acute: nearly half of primary forests were lost between 1996-2020 due to fire, logging, and hurricanes (Hong et al., 2025). Broader satellite definitions indicate 10-32% tree cover across the country, concentrated in protected areas such as Pic Macaya and La Visite National Parks (Hong et al., 2025). Agricultural expansion into upland and marginal zones remains the dominant deforestation driver, while built-up areas - though small - have doubled since 2000 0.6 to 1.3%) (Pauleus & Aide, 2020). With roughly 25 of 30 watersheds severely deforested (UNDP, n.d.), Haiti's degraded landscapes heightens its sensitivity to storm-related landslides and flooding, contrasting with the reforestation-driven resilience trends in Cuba and the mixed, partially stabilizing trajectory observed in Jamaica.

7.2.1 Storm surge

One of the greatest challenges posed by hurricanes is the storm surge, whose powerful waves can batter coastal infrastructure, especially buildings not designed to withstand such forces, often causing extensive damage and, in severe cases, fatalities by drowning. They are the leading cause of fatalities from hurricanes (NOAA, n.d.b). Additionally, they can lead to extensive property loss, erosion of beaches and coastal habitat loss, undermining foundations of roads, railroads, bridges, buildings, and pipelines (US Climate Resilience Toolkit, n.d.; The Guardian, 2025). In general, storm surges today are higher than they would have been in 1900 due to global sea level rise (US Climate Resilience Toolkit, n.d.).

In Jamaica, storm surges of about 13ft were expected (CBS News, 2025b). Residents of Westmoreland (Jamaica) were warned to anticipate life-threatening storm surges on Oct 27 (Jamaica Information Service, 2025). Hospital residents were relocated on a higher floor (CBS News, 2025). Storm surges led to water level increase of 16ft (4.8 metres) in Black River, completely destroying coastal infrastructure (The Guardian, 2025; BBC, 2025).

7.3 Critical Systems

Melissa has impacted multiple critical systems in Jamaica, Cuba and Haiti with substantial consequences for the emergency response, the subsequent impacts and the overall capacity to recover from the disaster. The need for better preparedness of the Jamaican transport sector to weather extremes was outlined based on vulnerability assessment in a publication by USAID (Zermoglio & Scott, 2018). In recognition of Jamaica's large exposure to hurricanes, due to its low-lying coastal areas with 82% of population living within 5 km from the coast, the Jamaica Disaster Vulnerability Reduction Project was initiated to improve disaster and climate resilience (World Bank, 2025), specific adaptations in this project are described in more detail in section 7.5.2. As part of 'Smart Health Care Facilities in the Caribbean Project' investments were made to make the health system of Jamaica more resilient to climate extremes, including reinforcements of roofs of health centers (PAHO, 2023; PAHO).

Critical infrastructure affected by Melissa includes the energy sector, where in Jamaica 77% of the island was reported to experience power outage (CBS News, 2025). Nationally, over 500,000 residents were left without power (Reuters, 2025). In Cuba, the energy grid experienced widespread outages, on top of an ongoing energy crisis (AP News, 2024; Al Jazeera, 2024; The Guardian, 2025). These power outages complicate emergency response, e.g. through the disruption of

telecommunication, as was experienced in Cuba and reported by the state-owned telecommunication provider (ETECSA, 2025)

Mobility was also severely affected by Melissa, including airport shutdowns, road closures and affected seaports. In Jamaica, many roads were covered in mud (PBS News, 2025; ABC News, 2025) and the Cave River Bridge in the center of the island was reported to be flooded (ReliefWeb, 2025), delaying emergency response in the area. As of October 30th, 130 roads in Jamaica were blocked by debris (CBS News, 2025). The main port of Montego Bay, the second largest city in Jamaica that is on its north coast, has experienced substantial impacts as visible from satellite imagery (CNN, 2025). Ports are of critical importance for Caribbean islands and the infrastructure and regulatory bodies in the port of Kingston (Jamaica) were identified as insufficiently prepared for disaster in work by Johnson et al. (2025) following 2022 Hurricane Ian. In Jamaica, the Montego Bay Sangster International Airport closed ahead of the storm at noon on October 26th (MBJ Airports Limited, 2025) and remained closed following severe damages by Melissa, delaying the necessary emergency response. As of October 30th, most Jamaican airports are still closed, but the Ian Fleming International Airport and Norman Manley Airports are open (ReliefWeb, 2025).

Healthcare services are also critical systems that have experienced damages and disruptions. Multiple hospitals in Jamaica have closed, including the Black River Hospital in St. Elizabeth, the Noel Holmes Hospital in Hanover, and the Falmouth Hospital in Trelawny. (Jamaica Information Service, 2025; ReliefWeb, 2025). In Cuba, the Juan Bruno Zayas Clinical Hospital experienced severe damage (PBS News, 2025), thus limiting the ability to provide necessary care. Water, Sanitation and Hygiene (WASH) infrastructure has been severely impacted with health risk. Access pre-disaster has been high in Jamaica (estimates of 80 to 90%) (PAHO 2024) but significantly lower in Cuba (41%) (World Bank, 2022), and Haiti (51% (OCHA, 2022). Infectious diseases spread fast in shelter and overcrowded spaces (PAHO 2024) and water borne diseases such as Cholera are a concern the following weeks as outbreaks have been seen in the aftermath of hurricane Mathew in Haiti for example (Hulland et al., 2018). Other major public health concerns include the particularly severe disease Leptospirosis, transmitted through contaminated freshwater used for cooking bathing and contaminated soil in contact with wounds. High case fatality rate requires timely treatment, severely hindered with disruption of services. (PAHO 2024).

7.4 Livelihoods and food security

Melissa has and will continue to have severe impacts on people's livelihoods, particularly in agriculture, fishing, and tourism. In Jamaica, besides hotels and tourist infrastructure, St. Elisabeth, Jamaica's breadbasket, and remote fishing communities such as White House have been heavily impacted or destroyed (BBC, 2025, CNN, 2025). In Haiti and Cuba, fields were submerged and livestock washed away (Tageschau, 2025, Washington Post, 2025).

Agriculture and tourism are important pillars of Jamaica's, Cuba's, and Haiti's economies, affecting local economies and exports broadly, requiring extensive recovery (Hidalgo et al., 2025, USDA, 2024, UN Stats, 2023). To exemplify, 20% of Jamaica's GDP relies on tourism and agriculture alone, and over half of all economic assets are located in the affected coastal areas (UN Stats, 2023, Statistical institute of Jamaica, 2019, Lee et al., 2022). However, past recovery prioritized tourism infrastructure while neglecting agriculture, fisheries, and critical systems, creating unequal recovery pathways (Sheller, 2021).

Recovery will need to be extensive after devastating impacts adding onto the devastation from Hurricane Beryl in 2024. St. Elizabeth's agricultural communities had not yet recovered in income, property, and land, and still experienced emotional distress a few months before Melissa (Smith, 2025). Farmers describe hesitancy to resume agricultural practices due to fear of another disaster, and hardship due to droughts throughout 2025 (Smith, 2025). They also face pre-existing vulnerabilities from lack of land ownership and difficulties accessing seeds and planting materials (Fath et al., 2018). Meanwhile fishing communities experience increasing pressures from declining and overexploitation of nearshore fish populations, beach erosion, repeated flooding and fragile fishing infrastructures (Campbell and Lee, 2021, Epstein et al., 2022 , National Environment and Planning Agency Jamaica, 2021).

Consequently, livelihoods have been shifting from agriculture to tourism across Caribbean islands in recent decades, but agriculture and fisheries remain important for local food security that is now threatened (Baker, 2017, Campbell and Lee, 2021). Already in January, Jamaica has been grappling with high food inflation (7.4%), and people reported skipping meals (World Food Programme, 2025). Yet, food insecurity in Jamaica is relatively low at 7.7%, compared to over 50% in Haiti and 37.8% in Cuba (FAO, 2025, USDA, 2024). As Melissa's full extent becomes clear, so will long-term consequences for food security and livelihoods.

7.5 Storm risk management

Most countries in the Caribbean are acutely aware of their hurricane risk and have a series of mechanisms to reduce them, prepare for disasters, and minimise losses and damages. In Jamaica there is a systemic, layered approach to storm risk management which includes: risk identification and mapping, a hurricane early warning and action system, adaptation projects, insurance and financial instruments.

Jamaica's disaster management is governed by the Disaster Risk Management Act 2015 and is coordinated by the Office of Disaster Preparedness and Emergency Management (ODPEM).

Cuba has a multi-layered disaster management programme with a strong civil defense system and active involvement at the community level including education, prevention and preparedness activities such as nationally mandated training drills for natural hazards (CIP, 2013).

7.5.1 Early warning and early action

The Meteorological Service of Jamaica is the primary agency which provides early warning alerts during hydrometeorological hazards, including hurricane watches and warnings. The ODPEM, in coordination with the Met. Office and other agencies use these alerts to issue evacuation orders and other early actions. Based on the forecast of Hurricane Melissa, the National Emergency Operations Centre (NEOC) was activated, which coordinated preparedness actions and emergency services, including evaluations amongst a range of stakeholders such as municipal corporations, Jamaica Defence Force, Jamaica Constabulary Force, Jamaica Fire Brigade, Jamaica Red Cross, UNDP and others (JIS, 2025). Jamaica's Disaster Risk Management system is three tiered, with parish and community systems supporting the national level. At

the local level, many communities have disaster risk management plans that map hazards and vulnerability and dictate emergency response roles and shelter management. Parish-level disaster coordinators are in touch with the NEOC and support implementation at the local level, along with community emergency response teams that are trained in first aid, shelter management, light search and rescue and disaster response capabilities, ensuring volunteers are available to respond.

7.5.2 Adaptation projects

The World Bank has a series of ongoing and completed projects in Jamaica, including a $7.5 million project to enhance climate related data and information for planning; a $30 million project to reduce vulnerability to disasters, and $4.88 million project to increase adoption of climate resilient practices in fishing and farming communities in Jamaica (GFDRR, 2025). As part of the vulnerability reduction project, for example, there was a component focused on reinforcing physical infrastructure including the rehabilitation of bridges and urban drainage; construction, rehabilitation and upgrading of fire stations; retrofitting of a school; and improving coastal protection (World Bank, 2024). In particular, they constructed three groynes in Annotto Bay, St. Mary, and extended the width of the beach by 12 meters seaward and raised the beach's height to 6 feet above mean sea level, with the aim of reducing erosion and inland flooding (World Bank, 2024). While it is too early to know at the time of writing, it would be valuable to check whether the infrastructure that was reinforced through this project did indeed fare better during this hurricane. Further, the same project supported the adoption of the Jamaica Fire Code, Jamaica Building Code, and Jamaica Small Building/Residential Code that would ensure that buildings meet national and international standards for resilience to climate-related disasters (World Bank, 2024).

There are also a series of nature-based solutions that are in place in various parts of Jamaica, including the restoration of mangroves, reforestation among others, some of which have been implemented by the Jamaica Red Cross and partners, such as The Nature Conservancy (TNC), under Initiatives such as The Resilient Islands Project (2018-2023) and the Greening Disaster Risk Reduction Project: Saving Lives through Working with Nature Project (2021-2025).

However, the intensity of Hurricane Melissa as a very strong category 5 storm is likely to lead to a level of destruction that is beyond what it is reasonably possible for a country to fully adapt to, leading to residual losses and damages.

7.5.3 Insurance and financial instruments

For Small Island States like Jamaica, disasters can be fiscally ruinous, with damages often encompassing a large proportion of annual GDP. For example, Hurricane Gilbert in 1988 led to damages that were approximately 30 percent of Jamaica's GDP at the time (Ministry of Finance, 2021). To avoid this, Jamaica has a series of insurance instruments and financial products designed to help protect the population in case of a hurricane that causes significant damage. The National Natural Disaster Risk Financing (NNDRF) policy guides Jamaica to have a multi-layer risk approach to financing disaster risk, which includes disaster risk insurance, contingent lines of credit, and contingent budgets, reserves, and annual budget allocations (Ministry of Finance, 2021). For example, Jamaica has a 150 Million USD catastrophe bond that provides insurance coverage for the

Government of Jamaica in the case of a named storm with a parametric trigger based on the minimum central pressure and storm location (World Bank, 2024). According to early indications, Hurricane Melissa made direct landfall with a central pressure of 892mb, which is likely to result in a full payout of $150 Million to support recovery (Artemis, 2025). Jamaica is also a part of the Caribbean Catastrophe Risk Insurance Facility (CCRIF) which includes parametric insurance based on losses due to wind and storm surge (CCRIF, 2025). And it has pre-arranged lines of credit with the Inter-American Development Bank and the World Bank that will provide it with liquidity to support a rapid recovery process (E&E News, 2025). Together, these instruments should support Jamaica in the immediate recovery phase, but the total financial impact of Melissa is preliminarily estimated to be nearly 8 Billion USD, reflecting a clear mismatch between the funds available and damages (Bloomberg, 2025).

7.6 Preparedness and Response

7.6.1 - Forecasting

Tropical Storm Melissa was announced in a public advisory on October 21st, 2025 by the United States National Hurricane Center (NHC). A hurricane watch was issued for Haiti and heavy rainfall was forecasted for Haiti and the Dominican Republic with the potential of landslides and flash flooding. The Meteorological Service of Jamaica (MSJ) issued a Tropical Storm Watch for Jamaica and its Office of Disaster Preparedness and Emergency Management (ODPEM) cautioned the public in flood and landslide prone areas of potential impacts. (JIS, NHC). The storm was monitored throughout October 22nd with updated forecasts and on October 23rd a Hurricane Watch was issued for Jamaica and southwestern Haiti, along with a Tropical Storm Warning. Although heavy rainfall was forecast in the Dominican Republic, Haiti and Jamaica, and storm surge for Jamaica, the path of the storm remained uncertain. (NHCa). On Friday October 24th 2025, forecasts predicted a rapid intensification of Melissa over the weekend, along with 'life-threatening and catastrophic flash flooding and landslides" in southern Hispaniola and Jamaica. (NHCb) At 11pm EST, the MSJ issued a Hurricane Warning for Jamaica, the NHC reiterated the likelihood of rapid intensification following NOAA and Airforce Reserve Hurricane Hunter flights. (NHCc,) On October 25th, the Government of Cuba issued a Hurricane Watch for parts of Cuba. (NHCd) On October 26th the Government of Cuba issued a Hurricane Warning for parts of the island. (NHCe) On October 27th a Tropical Storm Warning was issued for Haiti and Hurricane Melissa reached category 5 intensity levels. The government of the Bahamas issued a Hurricane Watch for the central and southeastern Bahamas as well as Turks a Caicos islands (NHCf, NHCg, NHCh).

7.6.2 - Preparedness measures

At 7.15am October 27th 2025, Jamaican officials issued a mandatory evacuation order for low-lying areas of Jamaica, specifically: 'Port Royal in Kingston; Portland Cottage and Rocky Point in Clarendon; Old Harbour Bay in St. Catherine; and New Haven, Riverton City and Taylor Land in St. Andrew'. This followed an address to the nation by the Prime Minister delivered on October 26th (ODPEM, ODPEMa) By evening on October 27th, as reported by the New York Times, Jamaica's Minister of Local Government warned that not enough residents were heading evacuation orders, with only 1,700 people in shelters. Government officials and independent experts cited possible barriers ranging from: challenges with evacuation infrastructure, disaster misinformation, the scale of forecasted intensity and reach across the island, risk perception and individual property protection.

(NYTa, NYTc, CNN) As of October 28th authorities in Jamaica had opened 881 shelters with approximately 6,000 people in them in advance of the storm, leaving many shelters largely empty according to the New York Times. (NYTb, BBC) The number of people reported in shelters grew to 15,000 just after landfall, according to Jamaica's Minister of Local Government, as reported by CNN. (CNNa).

In coordination with the Government, the humanitarian sector began pre-positioning stocks and activating coordination mechanisms early in the hurricane season (ECHO). In advance of the storm the Jamaican Red Cross activated volunteers at the national, parish and local levels, including its Community Disaster Response Teams (CDRT), prepositioned emergency relief stocks, aided in opening emergency shelters and facilitated evacuations. The IFRC released 80,000 CHF to help fund these pre-disaster, emergency preparedness actions. (IFRC) Schools were also moved online, Jamaica's main international airports were closed and cruise ships diverted to other locations. (BBCa, Carnival, Miami Herald) Hospitals also made various preparedness measures, even when limited options existed, for example moving patients to higher floors. (NYTg)

Hurricane Melissa made landfall in Santiago de Cuba on October 29th 2025 as a Category 3 Hurricane. (NHCi) More than 735,000 people were evacuated in advance of Hurricane Melissa's landfall, according to the Cuban President, as reported by CNN (CNNb). The Cuban Red Cross aided in those evacuations. (IFRCa) An OCHA-facilitated anticipatory action framework was activated to pre-position emergency relief supplies in Cuba and in Haiti. (OCHA, 2025).

As reported in the Haitian Times, on October 25th the Government of Haiti issued a Red Alert for Grand'Anse and Sud with orange alerts in effect for Southeast, Nippes and West. (Haitian Times) The Haitian Red Cross activated its Jérémie Emergency Operations Centre, to support coordination of pre and post-disaster actions, and volunteers shared information and guidance with families on how to protect themselves. (IFRCa) WFP provided anticipatory cash payments to approximately 50,000 people to help protect their livelihoods. (WFP)

7.6.3 - Response measures

The Jamaican Prime Minister issued a disaster declaration on October 28th. (OPM) The day before on October 27th, Jamaican authorities activated the Union Civil Protection Mechanism on October 27th, which facilitates emergency response support from the European Union. (ECHOa) IOM, WFP and IFRC dispatched an early release of emergency relief supplies from their regional stocks on October 28th and 29th 2025. (IOM, IFRC) Officials reported coordination efforts to facilitate the flow of emergency relief supplies, for example at ports and issuing a directive to prevent price gauging. (NYTd, NYTe) In the immediate aftermath of Hurricane Melissa, response efforts in Jamaica face physical access limits due to debris, and damage to power and communication infrastructure. More than 530,000 people were without power on October 28th, 2025 (CNNc). Extreme heat and humidity following the hurricane is also impacting response and clean-up efforts with a heat index over 100 degrees Fahrenheit (37.8 celsius) (CNN, 2025) On October 29, 2025, the Jamaican Government announced that all 25,000 tourists in Jamaica were accounted for. (NYTf). As of November 1st 2025, as reported by Al Jazeera, approximately 60% of Jamaicans remained without power and nearly half of water systems were still offline. (Al Jazeera) As of November 3rd the Jamaican Government had also activated additional response mechanisms such as a Hurricane Melisa volunteer registry, a national clean-up program, and an aid accountability mechanism. (Gleaner, Gleaner-a, Gleaner-b) A

situation report released on November 2nd by the Pan American Health Organization, in support of the Ministry of Health and Wellness of Jamaica, notes severe impacts to Jamaica's health system in the affected region, including five major hospitals being severely impacted. (PAHO) In addition to national relief efforts, international assistance has been offered by: EU, France, Luxemburg, Belgium, German, Japan, US, IFRC, WFP, among others (Japan, EU, ECHO, WFP, IFRC, CBS).

In Cuba, preliminary reports indicated significant damage to buildings and roads with over 900,000 buildings impacted to some degree, 200,000 of which were affected more substantially. (IFRCa) As reported by UNOCHA, additional impacts span across electricity, water supply, and telecommunications. Nearly 600 schools have been damaged and 287 health facilities. National relief efforts by the government, as reported by UNOCHA, in the first days of the response include damage assessments, restoration of core services (electricity, water, sanitation, telecommunications) and distribution of food, hygiene kits and fuel sources (Reliefweb). In addition to national relief efforts, international assistance has been committed by the EU, Venezuela, China, Colombia and Mexico; as well as UN partners such as WFP, UNDP and UNICEF (Reliefweb, EC, EU). An offer of assistance was made by the US (Reuters).

At the time of this study's release, response and recovery efforts are still in the early phases of what will be a much longer period given the severe impacts across the affected areas. In the days to come, more impacts will also emerge. Health impacts, especially from waterborne illnesses, are likely to grow, as water systems have been damaged, the risk for contaminated water grows daily, and the health system in the most affected areas is severely compromised. The magnitude of this hurricane and its rapid intensification points to some limits to adaptation, which should be explored in further studies. In the months and years ahead after action reviews, evaluations and future hazards will provide a clearer picture on the damage, preparedness and response actions, and lessons for future disasters.

7 Conclusions

Overall, it is clear that the rainfall, wind speeds from and conditions leading to Hurricane Melissa have all increased due to climate change. In particular, winds have become robustly more likely and intense, Jamaica and eastern Cuba are experiencing more intense extreme rainfall and we expect this to continue as the world warms further, and the potential intensity conditions leading to such an event will continue to become more intense (table 7.1).

Variable	Influence of Global Warming of 1.3C		
	Qualitative attribution (increase/decrease/no change)	Quantification	
		Probability ratio (95% C.I.)	Change in intensity (95% C.I.)
Extreme rainfall	Increase	N/A	>9%*
Wind speeds	Increase	**4.8 (2.6 to 9.6)**	**+5.1 m/s (+2.3 to 8.1 m/s)**
Environmental	Increase	**6.06**	**+2.65 m/s**

conditions (PI)		**(1.50 to 34.0)**	**(+0.91 to 4.31 m/s)**

Table 7.1: *Headline findings from hazard analyses from tables 5.1-5.3 and conclusions from section 5. *The quantification for rainfall is based on a combination of analysis in this report, wider physical understanding and other attribution studies, and therefore does not have 95% confidence intervals.*

It is therefore also overwhelmingly likely that the impacts of Hurricane Melissa were more severe as a result of climate change. These impacts were complex and occurred over multiple regions in different ways. Additionally, individual variables such as wind may drive impacts in different ways, such as through direct damage and driving storm surge, which may then compound rainfall-based flooding. In particular, while the changes in the magnitude of wind speeds seem small (~5 m/s), the damage potential of wind in the region of category 5 storms scales with the cube of intensity. Even small changes can therefore result in substantial increases in damage potential. It is also clear that the Caribbean has received far less attention than the mainland US in assessments of how climate change is influencing hurricanes now and with further warming (Vosper et al., 2020)

Jamaica, like many small island states, faces potentially catastrophic economic losses from hurricanes that have in the past been a large percentage of the country's GDP. For example, Hurricane Gilbert in 1988 led to damages that were approximately 30 percent of Jamaica's GDP at the time (Ministry of Finance, 2021). To mitigate such risks, the government employs a multi-layer financial strategy, including disaster risk insurance, catastrophe bonds, parametric insurance through the Caribbean Catastrophe Risk Insurance Facility (CCRIF), and pre-arranged lines of credit with the World Bank and Inter-American Development Bank. For example, Jamaica has a 150 Million USD catastrophe bond that provides insurance coverage for the Government of Jamaica in the case of a named storm with a parametric trigger based on the minimum central pressure and storm location (World Bank, 2024). Despite these measures, preliminary estimates suggest damages from Melissa are at least an order of magnitude larger than available finance, representing a proportion of GDP or even a factor of GDP, posing a huge strain on the country. Further, there are psycho-social and other nonfinancial impacts that are not easily quantified or included in these figures, but require acute attention.
In addition, Hurricane Melissa struck a year after Hurricane Beryl made landfall in the same region, devastating agriculture and fishery communities and further damaging infrastructure that had not yet recovered. To exemplify, 20% of Jamaica's GDP relies on tourism and agriculture alone, and over half of all economic assets are located in the affected coastal areas (UN Stats, 2023, Statistical institute of Jamaica, 2019, (Lee et al., 2022). However, past recovery prioritized tourism infrastructure while neglecting agriculture, fisheries, and critical systems, creating unequal recovery pathways (Sheller, 2021).

Forecasts of Melissa were available more than a week before landfall in both Jamaica and Cuba, allowing ample time for preparedness. In Cuba, over 735,000 people were evacuated from low-lying and coastal areas, while in Jamaica, 881 emergency shelters were opened, evacuations carried out, supplies pre-positioned, and transport operations suspended. These actions likely saved many lives. However, an event of such intensity highlights the soft limits of adaptation, particularly for infrastructure, showing that even strong preparedness measures cannot fully prevent severe impacts.

Data availability

All time series used in the attribution analysis are available via the Climate Explorer.

References

All references are given as hyperlinks in the text.

Appendix

A.1 Data and Methods

A.1.1 Observational and reanalysis data

In this study, we use several observational and reanalysis datasets to characterise Hurricane Melissa:

1. **MSWX -** The Multi-Source Weather dataset (Beck et al., 2022), which combines various observational and reanalysis-based data (including ERA5) for reliable bias-corrected weather variable estimates, at 3-hourly intervals from 1979 to near real-time, and at 0.1° spatial resolution globally. We use precipitation data from this product.
2. **CHIRPS -** The rainfall product developed by the UC Santa Barbara Climate Hazards Group called "Climate Hazards Group InfraRed Precipitation with Station data" (CHIRPS; Funk et al. 2015). Daily data are available at 0.05° resolution, from 1981-30 September 2025. The product incorporates satellite imagery with in-situ station data.
3. **ERA5 -** The European Centre for Medium-Range Weather Forecasts's 5th generation reanalysis product, ERA5, is a gridded dataset that combines historical observations into global estimates using advanced modelling and data assimilation systems (Hersbach et al., 2020). We use sea surface temperatures (SSTs), sea level pressure, and specific humidity and atmospheric temperatures at all available pressure levels from this product, at a resolution of 0.5°, from the years 1950 to present. The Potential Intensity is calculated from these variables using the open-source PyPI package (Gilford, 2021).

As a measure of anthropogenic climate change we use the (low-pass filtered) global mean surface temperature (GMST), where GMST is taken from the National Aeronautics and Space Administration (NASA) Goddard Institute for Space Science (GISS) surface temperature analysis (GISTEMP, Hansen et al., 2010 and Lenssen et al. 2019).

We also use the high-resolution blended analysis of daily SST and ice (DOISST v2.0) from the National Oceanic and Atmospheric Administration (NOAA). This is a blend of in-situ and buoy SSTs with satellite SSTs. Daily data is from NOAA PSL, Boulder, Colorado, USA, from their website at https://psl.noaa.gov, and is available from September 1981 to near-present at 0.25° resolution (Huang et al., 2021).

To model multidecadal variability in sea surface temperatures in the North Atlantic basin we use the Atlantic Multidecadal Variability (AMV). This is computed from NOAA's ERSST v.5 sea surface temperatures, by first taking the monthly average SSTs from 0°-60°N, 0°-80°W, and subtracting the monthly mean of the SSTs from 60°S-60°N to remove the global warming trend (Trenberth & Shea, 2006). The monthly values are first decadally smoothed using a rolling 121-month mean, and then averaged per calendar year to obtain an annual time series.

A.1.1.1 Reanalysis data performance

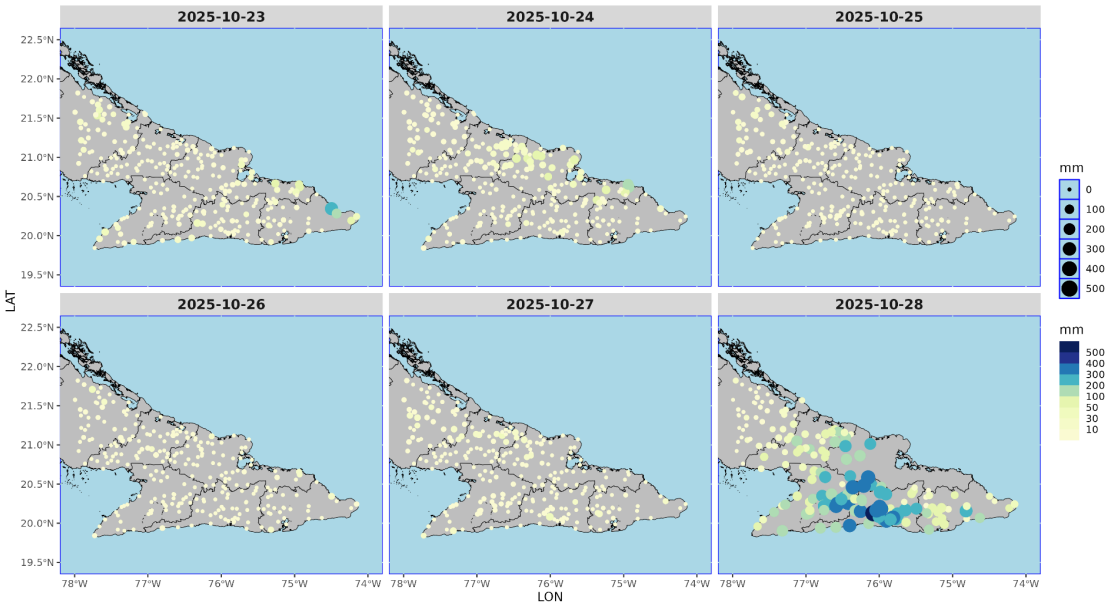

Figure A1: *Preliminary daily observations of rainfall from rain gauges across eastern Cuba (prior to quality control processes). Data from the Institute of Water Resources Informative Network (https://www.hidro.gob.cu).*

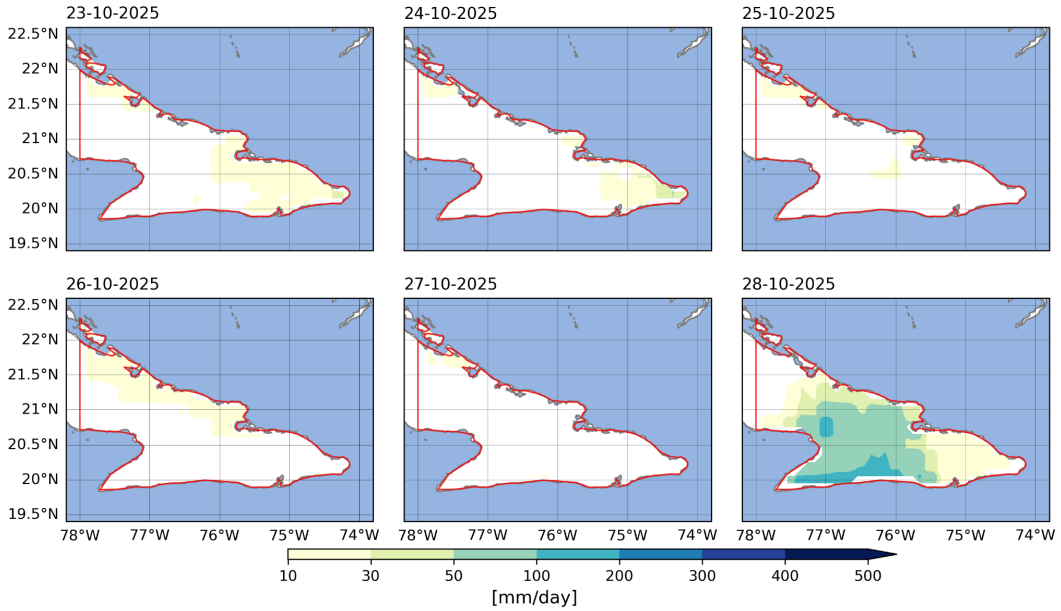

Figure A2: *Daily precipitation in MSWX gridded data, over the same region and on approximately the same visual colour scale as the preliminary observations shown in Fig.A1.*

A.1.2 Climate models

For analysis of extreme rainfall, we use 3 multi-model ensembles from climate modelling experiments using very different framings (Philip et al., 2020): Sea Surface temperature (SST) driven global circulation high resolution models, coupled global circulation models and regional climate models. These include:

1. Coordinated Regional Climate Downscaling Experiment (**CORDEX**) - Central America (CORDEX-CAM) data archive contains output from regional climate models (RCMs) run over a domain covering Central America using boundary conditions from global climate model (GCM) simulations in the CMIP5 archive. These simulations run from 1950–2100 with a spatial resolution of 0.22°/25km or 0.44°/50km (Cabos et al., 2018), composed of historical simulations up to 2005, and extended to the year 2100 using the RCP8.5 scenario.

2. The **FLOR** (Vecchi et al., 2014) and **AM2.5C360** (Yang et al., 2021, Chan et al., 2021) climate models are developed at Geophysical Fluid Dynamics Laboratory (GFDL). The FLOR model is an atmosphere-ocean coupled GCM with a resolution of 50 km for land and atmosphere and 1 degree for ocean and ice. Ten ensemble simulations from FLOR are analysed, which cover the period from 1860 to 2100 and include both the historical and RCP4.5 experiments driven by transient radiative forcings from CMIP5 (Taylor et al., 2012). AM2.5C360 is atmospheric GCM based on that in the FLOR model (Delworth et al., 2012, Vecchi et al., 2014) with a horizontal resolution of 25 km (and is referred to as 'AM2' throughout this text). Three ensemble simulations of the Atmospheric Model Intercomparison Project (AMIP) experiment (1871-2100) are analysed. Radiative forcings are using historical values over 1871-2014 and RCP4.5 values after that. Simulations are initialised from three different pre-industrial conditions but forced by the same SSTs from HadISST1 (Rayner et al., 2003) after groupwise adjustments (Chan et al., 2021) over 1871-2020. SSTs between 2021 and 2100 are using the FLOR RCP4.5 experiment 10-ensemble mean values after bias correction.

3. We use 11 runs from the **HighResMIP SST-forced model ensemble** (Haarsma et al., 2016), the simulations for which span from 1950 to 2050. The SST and sea ice forcings for the period 1950-2014 are obtained from the 0.25° x 0.25° Hadley Centre Global Sea Ice and Sea Surface Temperature dataset that have undergone area-weighted regridding to match the climate model resolution. For the 'future' time period (2015-2050), SST/sea-ice data are derived from RCP8.5 (CMIP5) projections, and combined with greenhouse gas forcings from SSP5-8.5 (CMIP6) simulations (see Section 3.3 of Haarsma et al. (2016) for further details).

Furthermore, to estimate the influence of anthropogenic climate change upon the potential intensity in which Melissa occurred, we use the **CMIP6** multi-model ensemble. This consists of simulations from 16 participating models with varying resolutions. For more details on CMIP6, please see Eyring et al., (2016). For all simulations, the period 1850 to 2015 is based on historical simulations, while the SSP5-8.5 scenario is used for the remainder of the 21st century.

A.1.3 Statistical methods

Methods for observational and model analysis and for model evaluation and synthesis are used according to the World Weather Attribution Protocol, described in Philip et al., (2020), with supporting details found in van Oldenborgh et al., (2021), Ciavarella et al., (2021) and here. The key steps, presented in sections 3-6, are: (3) trend estimation from observations; (4) model validation; (5) multi-method multi-model attribution; and (6) synthesis of the attribution statement.

In this report we analyse time series of extreme precipitation across four study regions (Jamaica, eastern Cuba, southern Haiti, and southern Dominican Republic), as well as potential intensity across the Caribbean sea and western Atlantic ocean. The influence of GMST is estimated by fitting a nonstationary statistical model, using GMST as covariate.

For extreme rainfall, a nonstationary generalised extreme value (GEV) distribution is used to model the extreme indices, and the distribution is assumed to scale exponentially with the covariates, with the dispersion (the ratio between the standard deviation and the mean) remaining constant over time. This formulation reflects the Clausius Clapeyron relation, which implies that precipitation scales exponentially with temperature (Trenberth et.al., 2003, O'Gorman and Schneider 2009). For potential intensity, a nonstationary Gaussian distribution is used to model the index. In this case, the distribution is assumed to shift linearly with the covariate GMST, while the variance remains constant. The parameters of all statistical models are estimated using maximum likelihood.

For each time series we calculate the return period and intensity of the event under study for the 2025 GMST and for 1.3 °C cooler GMST: this allows us to compare the climate of now and of the preindustrial past (1850-1900, based on the Global Warming Index), by calculating the probability ratio (PR; the factor-change in the event's probability) and change in intensity of the event.

A.1.3.1 Use of additional covariates

Throughout this study, we also extend the statistical model to include additional covariates in order to test the relative influence of major modes of natural variability. For instance, in order to examine the effect of the AMV on potential intensity alongside that of increasing GMST, the location parameter of the distribution is assumed to depend linearly on both GMST and the AMV:

$$X \sim N(\mu, \sigma \mid \mu_0,\ \sigma_0, \alpha, \beta,\ T,\ V),$$

where X denotes the variable of interest, Potential Intensity (PI); T is the smoothed GMST; V is the annual AMV index, as defined in Section 2.1; μ_0 and σ_0 are the mean and standard deviation of the nonstationary distribution when T and V are zero; and α, β are the trends due to GMST and AMV, respectively. As a result, the location of the distribution has a different value in each year, determined by both the GMST and AMV states. Maximum likelihood estimation is used to estimate the model parameters, with

$$\mu = \mu_0 + \alpha T + \beta V \qquad \text{and} \qquad \sigma = \sigma_0.$$

Under this model, the effects of GMST and the AMV index are assumed to be independent of one another, so that the change in intensity due to GMST is unaffected by the change in intensity due to the AMV.

A.1.4 IRIS methods

Observations show that the relative intensity, defined as observed maximum intensity divided by the potential intensity, follows a robust uniform distribution. This drives the stochastic model lifetime maximum intensity. The landfall intensity is then a fraction of this lifetime maximum depending on the time to landfall. Tracks are based on IBTRACS observations. The original model description paper has been published (Sparks and Toumi, 2024). IRIS calculates basin and landfall wind speed intensity distributions from the location of LMI and the corresponding potential intensity at that location, based on observed tracks between 1980 and 2024.

There has been a recent observed global warming of about 1.0°C, putting the global mean temperature close to about 1.3°C above pre-industrial temperature at the time of Melissa. Regional and local prediction of absolute PI by climate models is problematic as they are known to have biases. Regional observed changes are difficult to distinguish from natural variability. We therefore make the assumption that the anthropogenic trend is the global zonal mean PI trend, and use the observed PI trend since 1979 from ERA-5 (figure A3). There is some warming from pre-industrial to 1979 for which we have incomplete potential intensity data. To estimate the pre-industrial potential intensity state we extrapolate backwards the current observed trends. This approach avoids the selection of any climate model. The method is simple and robust.

A parametric rain model has been integrated into IRIS to simulate the axisymmetric rain field of landfalling storms. The model adopts the idealised rain profile of R-CLIPER (Tuleya et al., 2007) which defines the axisymmetric rain using four parameters. Within IRIS, these four parameters are estimated through linear regression relationships involving storm and environmental predictors, with an added stochastic component. Validation results indicate that IRIS successfully reproduces the observed global return period curve of the maximum azimuthal mean rain rate at landfall (Figure A4).

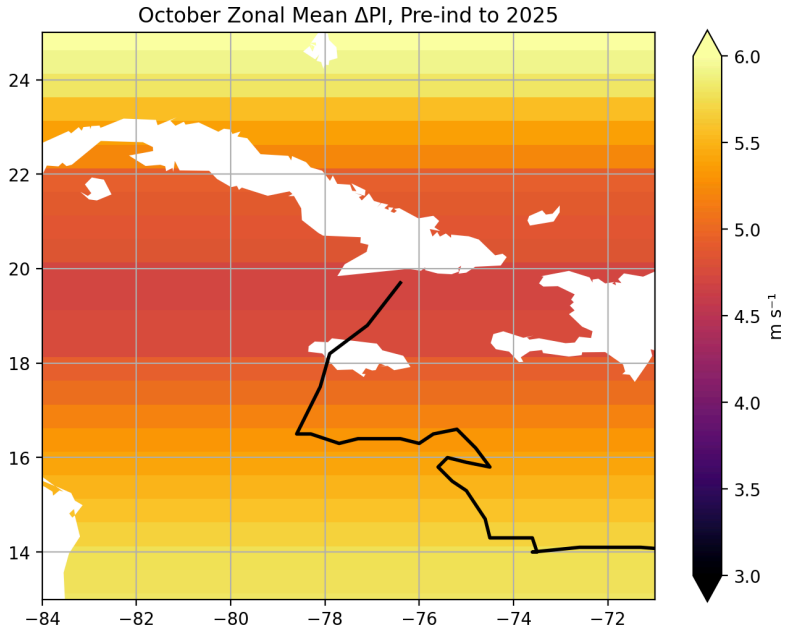

Figure A3: *Change in zonal mean potential intensity since pre-industrial conditions, based on the observed trend in ERA5 since 1979. The track of Melissa up to early on October 29th is shown in black.*

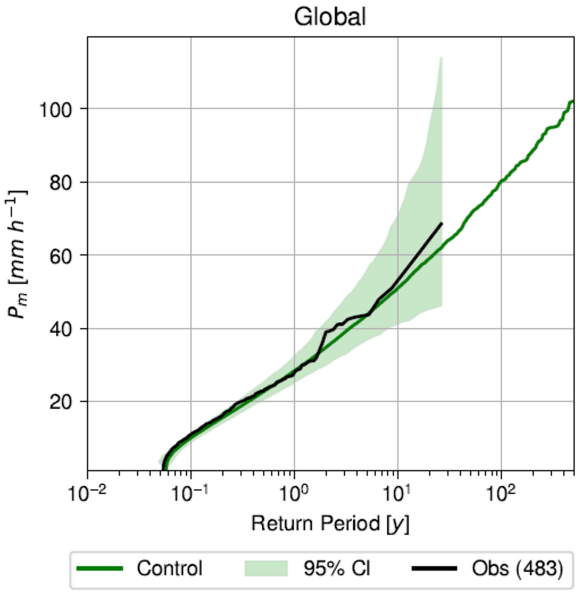

Figure A4: *Global validation of the IRIS model for the maximum azimuthal mean rain rate (mm/hr) at the last ocean point before landfall. Shown are return period curves from the 10,000-year IRIS control run (green) and from observations for 1998–2023 (black, with the number of events indicated in parentheses in the legend). The green shading indicates the 95% confidence interval, estimated from bootstrapping 1,000 26-year samples of the IRIS control run to match the observational record length.*

A.2 Sensitivity of observed rainfall trends

A.2.1 Seasonality

Dataset	Sep-Nov max 5-day rainfall		Trend with GMST	
	Magnitude (mm)	Return period (95% C.I.)	Probability Ratio	Change in magnitude (%)
Sep-Nov	519.7	39.0 (13.3 - 343.0)	**3.52** **(1.24 - 15.8)**	**63.8** **(7.59 - 133)**
June-Nov	519.7	39.4 (13.2 - 2163)	**3.99** **(1.29 - 633)**	**62.1** **(10.5 - 150)**

Table A1: *Observed magnitude and estimated return period in current climate conditions for the 5-day rainfall associated with Melissa in MSWX, considering June-November maxima and September-November maxima. Change in probability ratio and magnitude for* Rx5Day *in each case in Jamaica with increasing GMST are also shown. Statistically significant changes (at the 95% level) are shown in* ***bold text****.*

A.2.2 Observed trends by region

A.2.2.1 Jamaica, 2-day accumulations

Dataset	Jamaica 2-day rainfall		Trend with GMST	
	Magnitude (mm)	Return period (95% C.I.)	Probability Ratio	Change in magnitude (%)
MSWX	474.2	39.4 (11.4 - 203)	2.39 (0.76 - 6.13)	67.7 (-18.0 - 191)
CHIRPS	197.6	40	0.70 (10^{-6} - inf)	-8.39 (-63.4 - 97.7)

Table A2: *Observed magnitude and estimated return period in current climate conditions for the 2-day rainfall associated with Melissa in Jamaica, considering September-November maxima. Change in probability ratio and magnitude in Jamaica with increasing GMST are also shown. Highlighting in blue (orange) shows an increasing (decreasing) trend.*

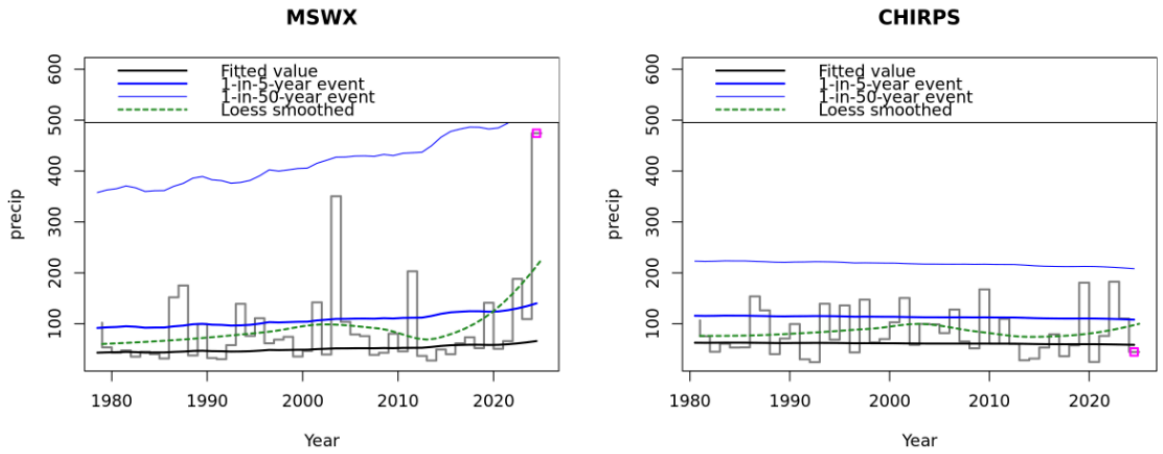

Figure A5: *Time series of September-November maxima of 2-day accumulated precipitation in Jamaica in MSWX (left) and CHIRPS (right). The modelled influence of GMST on the expected value (5- and 50-year return period values) is shown with the black line (bold and lighter blue lines), while the loess smoothed trend is shown with the green dashed line. The purple box shows the magnitude of the observed event in MSWX (left), and for CHIRPS (right) it shows the 2025 value which does not include the event itself.*

A.2.2.2 Eastern Cuba, 2-day accumulations

2days

Dataset	Eastern Cuba 2-day rainfall		Trend with GMST	
	Magnitude (mm)	Return period (95% C.I.)	Probability Ratio	Change in magnitude (%)
MSWX	135.1	16.0 (6.24 - 47.9)	2.02 (0.64 - 103)	36.7 (-26.1 - 176.6)
CHIRPS	129.9	15	9.61 (0.19 - inf)	57.1 (-24.1 - 177.6)

Table A3: *Observed magnitude and estimated return period in current climate conditions for the 2-day rainfall associated with Melissa in eastern Cuba, considering September-November maxima. Change in probability ratio and magnitude in Jamaica with increasing GMST are also shown. Highlighting in blue (orange) shows an increasing (decreasing) trend.*

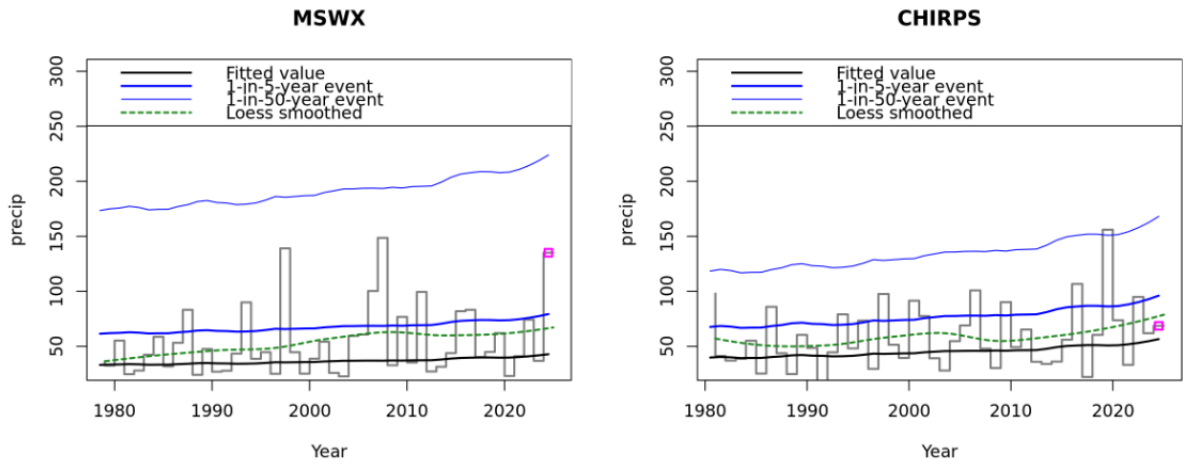

Figure A6: *Time series of September-November maxima of 2-day accumulated precipitation in eastern Cuba in MSWX (left) and CHIRPS (right). The modelled influence of GMST on the expected value (5- and 50-year return period values) is shown with the black line (bold and lighter blue lines), while the loess smoothed trend is shown with the green dashed line. The purple box shows the magnitude of the observed event in MSWX (left), and for CHIRPS (right) it shows the 2025 value which does not include the event itself.*

A.2.2.3 Haiti, full country accumulations

Dataset	Haiti 5-day rainfall		Trend with GMST	
	Magnitude (mm)	Return period (95% C.I.)	Probability Ratio	Change in magnitude (%)
MSWX	48.6	1.23 (1.02 - 1.79)	0.88 (0.57 - 1.23)	-15.0 (-46.4 - 47.1)
CHIRPS	81.3	2	0.95 (0.27 - 2.77)	-2.52 (-41.9 - 60.1)

Table A4: *Observed magnitude and estimated return period in current climate conditions for the 5-day rainfall associated with Melissa in Haiti averaged over the full country, considering September-November maxima. Change in probability ratio and magnitude in Jamaica with increasing GMST are also shown. Trends close to 'no change' are highlighted in grey.*

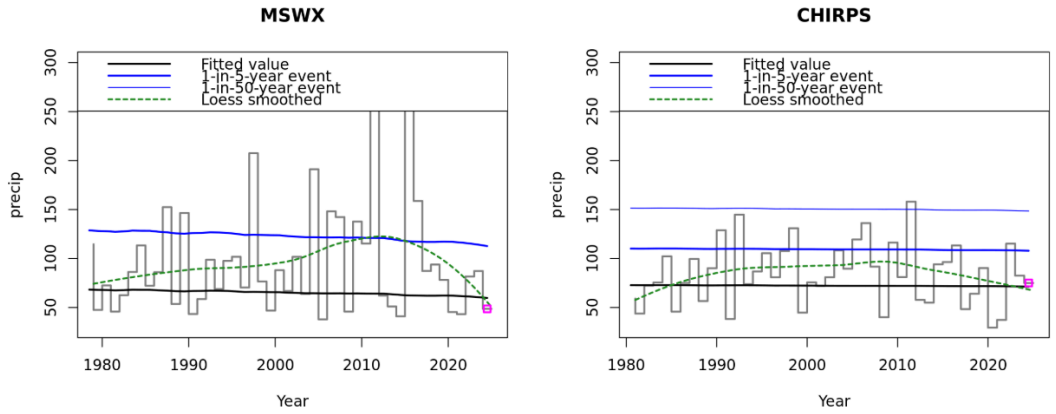

Figure A7: *Time series of September-November maxima of 5-day accumulated precipitation in Haiti in MSWX (left) and CHIRPS (right). The modelled influence of GMST on the expected value (5- and 50-year return period values) is shown with the black line (bold and lighter blue lines), while the loess smoothed trend is shown with the green dashed line. The purple box shows the magnitude of the observed event in MSWX (left), and for CHIRPS (right) it shows the 2025 value which does not include the event itself.*

A.2.2.4 Dominican Republic, full country accumulations

Full island

Dataset	Dominican Republic 5-day rainfall		Trend with GMST	
	Magnitude (mm)	Return period (95% C.I.)	Probability Ratio	Change in magnitude (%)
MSWX	90.7	3.69 (1.95 - 11.4)	0.97 (0.21 - 3.49)	-1.05 (-49.0 - 61.5)
CHIRPS	98.0	5	0.37 (0.039 - 1.32)	-31.2 (-62.0 - 12.2)

Table A5: *Observed magnitude and estimated return period in current climate conditions for the 5-day rainfall associated with Melissa averaged over the full Dominican Republic, considering September-November maxima. Change in probability ratio and magnitude in Jamaica with increasing GMST are also shown. Trends close to 'no change' are highlighted in grey.*

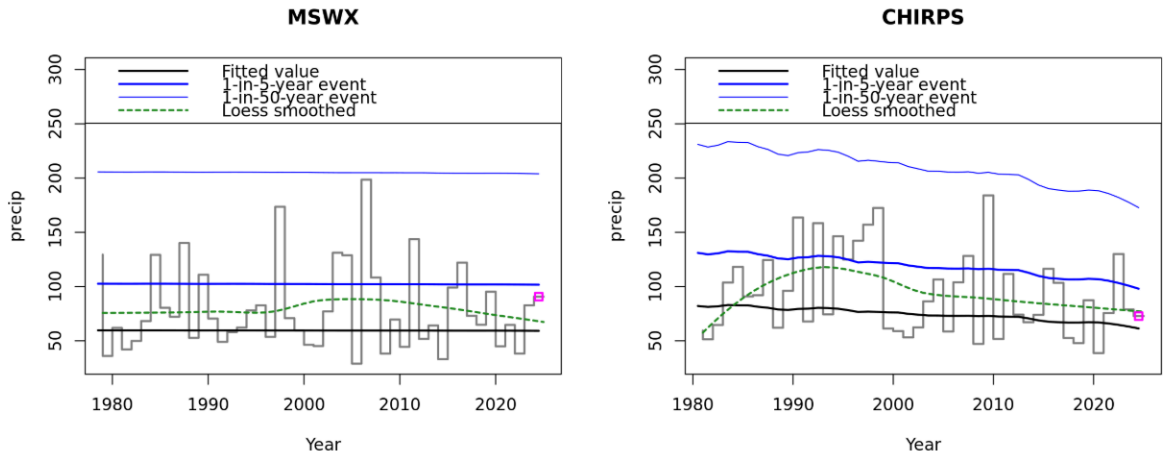

Figure A8: *Time series of September-November maxima of 5-day accumulated precipitation in the Dominican Republic in MSWX (left) and CHIRPS (right). The modelled influence of GMST on the expected value (5- and 50-year return period values) is shown with the black line (bold and lighter blue lines), while the loess smoothed trend is shown with the green dashed line. The purple box shows the magnitude of the observed event in MSWX (left), and for CHIRPS (right) it shows the 2025 value which does not include the event itself.*

A.3 Model evaluation

In this section we show the results of the model evaluation for the assessed region. The climate models are evaluated against the observations in their ability to capture:

1. Seasonal cycles: For this, we qualitatively compare the seasonal cycles based on model outputs against observations-based cycles. We discard the models that exhibit ill-defined peaks in their seasonal cycles.

2. Spatial patterns: Models that do not match the observations in terms of the large-scale precipitation patterns are excluded. In this case, the models should resolve distinct islands across the Caribbean, which largely depends on horizontal resolution and treatment of topography.

3. Parameters of the fitted statistical models. We discard the model if the model and observation parameters ranges do not overlap.

The models are labelled as 'good','reasonable', or 'bad' based on their performances in terms of the three criteria discussed above. A model is given an overall rating of 'good' if it is rated 'good' for all three characteristics. If there is at least one 'reasonable', then its overall rating will be 'reasonable' and 'bad' if there is at least one 'bad'. Per framing or model setup we also use models that only just pass the validation tests if we only have five models or less for that framing that perform well. The tables show the model validation results.

A.3.1 Extreme rainfall

A.3.1.1 Jamaica

Table A6: *Evaluation results of the climate models considered for attribution analysis of Rx5day. For each model, the threshold for a 1-in-40-year event is shown, along with the best estimates of the Dispersion and Shape parameters are shown, along with a 95% confidence intervals. Furthermore evaluation of the seasonal cycle and spatial pattern are shown.*

Model / Observations	Seasonal cycle	Spatial pattern	Dispersion	Shape parameter	Conclusion
MSWX			0.411 (0.281 ... 0.496)	0.39 (0.12 ... 0.84)	
CHIRPS			0.493 (0.371 ... 0.550)	0.19 (-0.15 ... 0.60)	
CORDEX					
CAM-22_CanESM2_r1i1p1_CRCM5	bad	reasonable	0.284 (0.219 ... 0.340)	0.26 (-0.13 ... 0.52)	bad
CAM-22_CNRM-CM5_r1i1p1_CRCM5	good	good	0.502 (0.374 ... 0.586)	0.31 (0.041 ... 0.92)	good
CAM-22_GFDL-ESM2M_r1i1p1_CRCM5	reasonable	good	0.448 (0.353 ... 0.543)	0.64 (0.30 ... 0.92)	reasonable
CAM-22_GFDL-ESM2M_r1i1p1_RegCM4-7	reasonable	good	0.269 (0.217 ... 0.317)	0.28 (-0.0043 ... 0.56)	reasonable
CAM-22_HadGEM2-ES_r1i1p1_RegCM4-7	good	good	0.420 (0.339 ... 0.486)	0.30 (-0.015 ... 0.66)	good
CAM-22_HadGEM2-ES_r1i1p1_REMO2015	good	bad	0.416 (0.280 ... 0.477)	0.40 (0.099 ... 1.1)	bad
CAM-22_MPI-ESM-LR_r1i1p1_REMO2015	good	bad	0.510 (0.415 ... 0.630)	0.047 (-0.59 ... 0.31)	bad
CAM-22_MPI-ESM-MR_r1i1p1_RegCM4-7	good	good	0.368 (0.296 ... 0.431)	-0.31 (-0.56 ... -0.094)	reasonable

CAM-22_NorESM1-M_r1i1p1_REMO2015	bad	reasonable	0.508 (0.408 ... 0.584)	0.39 (0.10 ... 0.71)	bad
CAM-44_CanESM2_r1i1p1_CRCM5	bad	reasonable	0.223 (0.157 ... 0.279)	0.020 (-0.69 ... 0.44)	bad
CAM-44_CanESM2_r1i1p1_RCA4	reasonable	good	0.174 (0.135 ... 0.204)	-0.13 (-0.59 ... 0.029)	bad
CAM-44_CNRM-CM5_r1i1p1_RCA4	reasonable	good	0.386 (0.293 ... 0.441)	0.34 (0.071 ... 0.58)	reasonable
CAM-44_CSIRO-Mk3-6-0_r1i1p1_RCA4	reasonable	good	0.168 (0.111 ... 1.46)	0.59 (0.062 ... 3.9)	reasonable
CAM-44_EC-EARTH_r12i1p1_RCA4	reasonable	good	0.366 (0.261 ... 0.417)	0.42 (-0.014 ... 1.0)	reasonable
CAM-44_GFDL-ESM2M_r1i1p1_RCA4	reasonable	good	0.277 (0.173 ... 0.345)	0.22 (0.019 ... 0.70)	reasonable
CAM-44_HadGEM2-ES_r1i1p1_RCA4	reasonable	good	0.333 (0.238 ... 0.398)	0.28 (-0.19 ... 0.58)	reasonable
CAM-44_HadGEM2-ES_r1i1p1_RegCM4-3	good	reasonable	0.545 (0.411 ... 0.628)	0.14 (-0.19 ... 0.35)	reasonable
CAM-44_HadGEM2-ES_r2i1p1_RegCM4-3	reasonable	bad	0.344 (0.286 ... 0.427)	0.19 (-0.044 ... 0.38)	bad
CAM-44_IPSL-CM5A-MR_r1i1p1_RCA4	reasonable	good	0.279 (0.216 ... 0.338)	-0.069 (-0.29 ... 0.19)	reasonable
CAM-44_MIROC5_r1i1p1_RCA4	reasonable	good	0.405 (0.318 ... 0.470)	0.25 (-0.23 ... 0.53)	reasonable
CAM-44_MPI-ESM-LR_r1i1p1_RCA4	reasonable	good	0.337 (0.262 ... 0.386)	0.21 (0.046 ... 0.38)	reasonable
CAM-44_MPI-ESM-MR_r1i1p1_RegCM4-3	reasonable	bad	0.468 (0.351 ... 0.530)	0.38 (-0.14 ... 0.68)	bad
CAM-44_NorESM1-M_r1i1p1_RCA4	bad	good	0.290 (0.209 ... 0.343)	-0.10 (-0.45 ... 0.18)	bad
HighResMIP					
CMCC-CM2-HR4_r1i1p1f1	reasonable	bad	0.388 (0.272 ... 0.454)	0.0090 (-0.28 ... 0.21)	bad
CMCC-CM2-VHR4_r1i1p1f1	good	good	0.473 (0.376 ... 0.522)	0.21 (-0.14 ... 0.58)	good
CNRM-CM6-1-HR_r1i1p1f2	reasonable	reasonable	0.309 (0.174 ... 0.362)	0.51 (0.26 ... 1.1)	reasonable
EC-Earth3P-HR_r1i1p1f1	good	good	0.296 (0.187 ... 0.368)	0.34 (0.14 ... 0.90)	good
EC-Earth3P_r1i1p1f1	reasonable	good	0.451 (0.383 ... 0.508)	0.066 (-0.33 ... 0.39)	reasonable
HadGEM3-GC31-HM_r1i1p1f1	good	good	0.347 (0.239 ... 0.424)	0.57 (0.30 ... 0.86)	good
HadGEM3-GC31-LM_r1i14p1f1	good	bad	0.471 (0.372 ... 0.551)	0.30 (0.084 ... 0.61)	bad
HadGEM3-GC31-MM_r1i1p1f1	good	bad	0.291 (0.218 ... 0.350)	0.39 (0.16 ... 0.86)	bad
MPI-ESM1-2-HR_r1i1p1f1	reasonable	bad	0.285 (0.233 ... 0.326)	-0.043 (-0.40 ... 0.28)	bad
MPI-ESM1-2-XR_r1i1p1f1	reasonable	bad	0.360 (0.289 ... 0.425)	-0.0091 (-0.54 ... 0.15)	bad
CNRM-CM6-1_r1i1p1f2	bad	bad			bad
AM2					
mem6	good	good	0.245 (0.187 ... 0.289)	0.32 (0.089 ... 0.60)	reasonable
mem7	good	good	0.270 (0.205 ... 0.304)	0.064 (-0.16 ... 0.25)	reasonable
mem8	good	good	0.365 (0.258 ... 0.469)	0.37 (0.16 ... 0.72)	good
FLOR					
mem1	reasonable	bad	0.342 (0.193 ... 0.408)	0.19 (-0.21 ... 0.59)	bad
mem2	reasonable	bad	0.392 (0.290 ... 0.485)	0.30 (-0.025 ... 0.52)	bad
mem3	reasonable	bad	0.473 (0.314 ... 0.596)	0.24 (0.022 ... 0.66)	bad
mem4	reasonable	bad	0.382 (0.309 ... 0.441)	0.19 (-0.43 ... 0.56)	bad
mem5	reasonable	bad	0.320 (0.217 ... 0.374)	0.24 (-0.23 ... 0.48)	bad
mem6	reasonable	bad	0.326 (0.245 ... 0.363)	0.31 (0.015 ... 0.63)	bad
mem7	reasonable	bad	0.366 (0.295 ... 0.415)	0.078 (-0.33 ... 0.47)	bad
mem8	reasonable	bad	0.397 (0.291 ... 0.469)	0.073 (-0.23 ... 0.37)	bad
mem9	reasonable	bad	0.317 (0.245 ... 0.365)	0.19 (-0.12 ... 0.46)	bad

mem10	reasonable	bad	0.317 (0.177 ... 0.379)	0.20 (-0.13 ... 0.67)	bad

A.3.1.2 Eastern Cuba

Table A7: *Evaluation results of the climate models considered for attribution analysis of Rx5day. For each model, the threshold for a 1-in-10 year event is shown, along with the best estimates of the Dispersion and Shape parameters are shown, along with a 95% confidence intervals. Furthermore evaluation of the seasonal cycle and spatial pattern are shown.*

Model / Observations	Seasonal cycle	Spatial pattern	Dispersion	Shape parameter	Conclusion
MSWX			0.347 (0.244 ... 0.403)	0.058 (-0.18 ... 0.58)	
CHIRPS			0.382 (0.250 ... 0.437)	0.091 (-0.19 ... 1.0)	
CORDEX					
CAM-22_CanESM2_r1i1p1_CRCM5	bad	reasonable	0.287 (0.217 ... 0.350)	0.38 (-0.087 ... 0.60)	bad
CAM-22_CNRM-CM5_r1i1p1_CRCM5	good	good	0.523 (0.402 ... 0.569)	0.31 (-0.084 ... 0.58)	reasonable
CAM-22_GFDL-ESM2M_r1i1p1_CRCM5	reasonable	good	0.356 (0.267 ... 0.458)	0.53 (0.034 ... 0.98)	reasonable
CAM-22_GFDL-ESM2M_r1i1p1_RegCM4-7	reasonable	good	0.324 (0.251 ... 0.380)	0.35 (-0.076 ... 1.1)	reasonable
CAM-22_HadGEM2-ES_r1i1p1_RegCM4-7	good	good	0.344 (0.270 ... 0.399)	-0.067 (-0.45 ... 0.33)	good
CAM-22_HadGEM2-ES_r1i1p1_REMO2015	good	bad	0.358 (0.272 ... 0.410)	0.36 (0.043 ... 0.89)	bad
CAM-22_MPI-ESM-LR_r1i1p1_REMO2015	good	bad	0.455 (0.321 ... 0.549)	0.22 (0.027 ... 0.51)	bad
CAM-22_MPI-ESM-MR_r1i1p1_RegCM4-7	good	good	0.331 (0.242 ... 0.400)	-0.15 (-0.53 ... 0.21)	good
CAM-22_NorESM1-M_r1i1p1_REMO2015	bad	reasonable	0.304 (0.209 ... 0.358)	0.36 (0.085 ... 0.79)	bad
CAM-44_CanESM2_r1i1p1_CRCM5	bad	reasonable	0.229 (0.193 ... 0.260)	-0.24 (-0.49 ... 0.0053)	bad
CAM-44_CanESM2_r1i1p1_RCA4	reasonable	good	0.220 (0.144 ... 0.273)	-0.29 (-0.58 ... 0.0095)	reasonable
CAM-44_CNRM-CM5_r1i1p1_RCA4	reasonable	good	0.492 (0.362 ... 0.569)	0.45 (0.21 ... 0.78)	reasonable
CAM-44_CSIRO-Mk3-6-0_r1i1p1_RCA4	reasonable	good	0.215 (0.165 ... 1.62)	0.50 (0.027 ... 3.6)	reasonable
CAM-44_EC-EARTH_r12i1p1_RCA4	reasonable	good	0.368 (0.292 ... 0.450)	0.50 (-0.022 ... 0.94)	reasonable
CAM-44_GFDL-ESM2M_r1i1p1_RCA4	reasonable	good	0.370 (0.287 ... 0.432)	0.13 (-0.19 ... 0.40)	reasonable
CAM-44_HadGEM2-ES_r1i1p1_RCA4	reasonable	good	0.323 (0.229 ... 0.366)	0.18 (-0.22 ... 0.42)	reasonable
CAM-44_HadGEM2-ES_r1i1p1_RegCM4-3	good	reasonable	0.610 (0.510 ... 0.678)	0.16 (-0.23 ... 0.72)	bad
CAM-44_HadGEM2-ES_r2i1p1_RegCM4-3	reasonable	bad	0.317 (0.228 ... 0.384)	-0.023 (-0.21 ... 0.31)	bad
CAM-44_IPSL-CM5A-MR_r1i1p1_RCA4	reasonable	good	0.280 (0.217 ... 0.316)	0.015 (-0.51 ... 0.25)	reasonable
CAM-44_MIROC5_r1i1p1_RCA4	reasonable	good	0.415 (0.279 ... 0.507)	0.31 (0.038 ... 0.70)	reasonable
CAM-44_MPI-ESM-LR_r1i1p1_RCA4	reasonable	good	0.397 (0.304 ... 0.463)	0.33 (-0.13 ... 0.73)	reasonable
CAM-44_MPI-ESM-MR_r1i1p1_RegCM4-3	reasonable	bad	0.425 (0.340 ... 0.492)	-0.092 (-0.43 ... 0.16)	bad
CAM-44_NorESM1-M_r1i1p1_RCA4	bad	good	0.326 (0.253 ... 0.376)	-0.0065 (-0.32 ... 0.33)	bad
HighResMIP					
CMCC-CM2-HR4_r1i1p1f1	reasonable	bad	0.388 (0.272 ... 0.454)	0.0090 (-0.28 ... 0.21)	bad
CMCC-CM2-VHR4_r1i1p1f1	good	good	0.473 (0.376 ... 0.522)	0.21 (-0.14 ... 0.58)	reasonable
CNRM-CM6-1-HR_r1i1p1f2	reasonable	reasonable	0.309 (0.174 ... 0.362)	0.51 (0.26 ... 1.1)	reasonable
EC-Earth3P-HR_r1i1p1f1	good	good	0.296 (0.187 ... 0.368)	0.34 (0.14 ... 0.90)	good

EC-Earth3P_r1i1p1f1	reasonable	good	0.451 (0.383 ... 0.508)	0.066 (-0.33 ... 0.39)	reasonable
HadGEM3-GC31-HM_r1i1p1f1	good	good	0.347 (0.239 ... 0.424)	0.57 (0.30 ... 0.86)	good
HadGEM3-GC31-LM_r1i14p1f1	good	bad	0.471 (0.372 ... 0.551)	0.30 (0.084 ... 0.61)	bad
HadGEM3-GC31-MM_r1i1p1f1	good	bad	0.291 (0.218 ... 0.350)	0.39 (0.16 ... 0.86)	bad
MPI-ESM1-2-HR_r1i1p1f1	reasonable	bad	0.285 (0.233 ... 0.326)	-0.043 (-0.40 ... 0.28)	bad
MPI-ESM1-2-XR_r1i1p1f1	reasonable	bad	0.360 (0.289 ... 0.425)	-0.0091 (-0.54 ... 0.15)	bad
CNRM-CM6-1_r1i1p1f2	bad	bad			bad
AM2					
mem6	good	good	0.238 (0.177 ... 0.274)	0.33 (-0.00072 ... 0.61)	reasonable
mem7	good	good	0.233 (0.114 ... 0.276)	0.26 (0.011 ... 1.1)	reasonable
mem8	good	good	0.272 (0.196 ... 0.322)	-0.077 (-0.34 ... 0.33)	good
FLOR					
mem1	good	bad	0.270 (0.184 ... 0.316)	0.076 (-0.14 ... 0.29)	bad
mem2	good	bad	0.231 (0.176 ... 0.267)	-0.15 (-0.44 ... 0.028)	bad
mem3	good	bad	0.246 (0.139 ... 0.284)	0.060 (-0.33 ... 0.47)	bad
mem4	good	bad	0.284 (0.206 ... 0.324)	0.025 (-0.19 ... 0.33)	bad
mem5	good	bad	0.256 (0.193 ... 0.299)	0.095 (-0.20 ... 0.34)	bad
mem6	good	bad	0.328 (0.174 ... 0.394)	0.10 (-0.064 ... 0.60)	bad
mem7	good	bad	0.272 (0.217 ... 0.313)	-0.19 (-0.38 ... 0.078)	bad
mem8	good	bad	0.245 (0.176 ... 0.291)	0.090 (-0.35 ... 0.38)	bad
mem9	good	bad	0.219 (0.147 ... 0.260)	0.028 (-0.12 ... 0.27)	bad
mem10	good	bad	0.243 (0.195 ... 0.279)	-0.22 (-0.55 ... -0.046)	bad

A.3.2 Potential Intensity

Of the 16 CMIP6 models analysed, 8 were rated ‘bad’ and discarded from the attribution analysis. No models performed well across all criteria, so all 8 remaining models were used.

Model / Observations	**Seasonal cycle**	**Spatial pattern**	**Sigma**	**Conclusion**
ERA5			2.29 (1.93 ... 2.56)	
CMIP6				
ACCESS-CM2_r1i1p1f1	reasonable	bad	3.14 (2.58 ... 3.57)	bad
BCC-CSM2-MR_r1i1p1f1	good	reasonable	2.05 (1.65 ... 2.34)	reasonable
CanESM5_r1i1p1f1	reasonable	reasonable	3.30 (2.74 ... 3.77)	bad
CanESM5-CanOE_r1i1p2f1	reasonable	reasonable	3.70 (2.82 ... 4.59)	bad
CMCC-CM2-SR5_r1i1p1f1	good	reasonable	2.85 (2.33 ... 3.24)	reasonable
CMCC-ESM2_r1i1p1f1	good	reasonable	2.19 (1.85 ... 2.44)	reasonable
E3SM-1-1_r1i1p1f1	good	reasonable	4.24 (3.53 ... 4.81)	bad
HadGEM3-GC31-LL_r1i1p1f3	good	bad	2.95 (2.39 ... 3.42)	bad
INM-CM5-0_r1i1p1f1	reasonable	bad	1.48 (1.16 ... 1.73)	bad

KIOST-ESM_r1i1p1f1	good	reasonable	3.11 (2.71 ... 3.40)	bad
MIROC6_r1i1p1f1	reasonable	reasonable	3.03 (2.55 ... 3.37)	reasonable
MPI-ESM1-2-LR_r1i1p1f1	good	good	3.63 (3.00 ... 4.13)	reasonable (good spatial)
NESM3_r1i1p1f1	reasonable	bad	3.04 (2.51 ... 3.44)	bad
NorESM2-LM_r1i1p1f1	good	good	3.58 (3.03 ... 3.96)	reasonable (good spatial)
TaiESM1_r1i1p1f1	good	reasonable	2.08 (1.67 ... 2.38)	reasonable
UKESM1-0-LL_r1i1p1f2	good	good	3.41 (2.81 ... 3.86)	reasonable (good spatial)

Table A8: *Evaluation of the climate models considered for attribution of potential intensity around the track of Hurricane Melissa. For each model, the best estimate of the sigma parameter is shown with a 95% confidence interval, obtained via bootstrapping. The qualitative evaluation is shown in the right-hand column.*

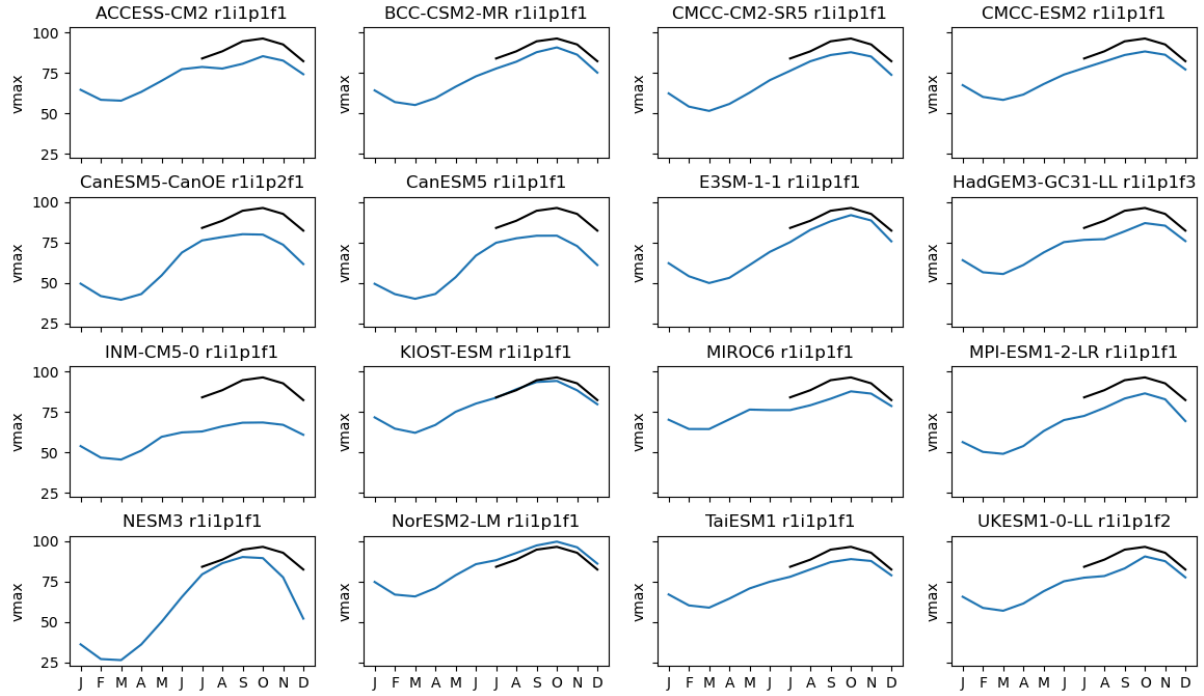

Figure A9: *Climatological (1991-2020) seasonal cycles of the monthly mean PI in the study region in CMIP6 climate models (blue line) and ERA5 (black line).*

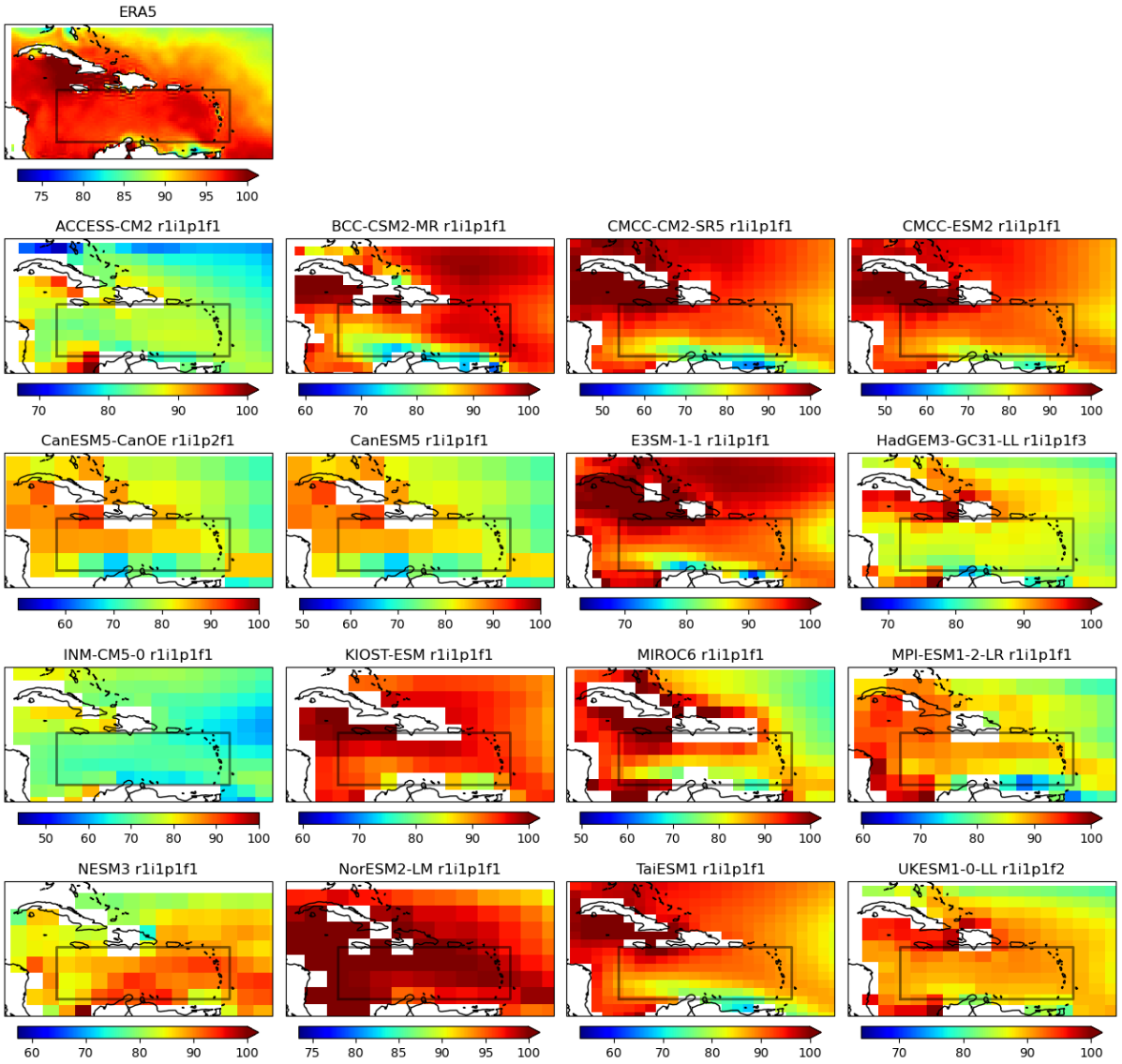

Figure A10: *Climatological (1991-2020) spatial patterns of the monthly mean PI in the study region in CMIP6 climate models and ERA5 (top left panel).*

A.4 Synthesis figures

For all of the event definitions described in sections 2 and 3, including extreme rainfall and potential intensity, we evaluate the influence of anthropogenic climate change on the event by calculating the probability ratio as well as the change in intensity using observations and climate models. The aim is to synthesise results from models that pass the evaluation along with the observations-based products, to give an overarching attribution statement. For full details of the method used to synthesise results from observations and climate models, see Otto et al. (2024).

Figures A11-A16 show the changes in probability and intensity for the observations (blue) and models (red). Before combining them into a synthesised assessment, first, a representation error is added in quadrature to the observations, to account for the difference between observations-based datasets that cannot be explained by natural variability. This is shown in these figures as white boxes around the light blue bars. The dark blue bar shows the average over the observation-based products. Next,a term to account for inter-model spread is added in quadrature to the natural variability of the models. This is shown in the figures as white boxes around the light red bars. The dark red bar shows the model average, consisting of a weighted mean using the (uncorrelated) uncertainties due to natural variability plus the term representing inter-model spread (i.e., the inverse square of the white bars). Where no finite estimate of the upper bound of an infinite is obtained, a finite upper bound is inferred by using the distance between the best estimate and lower bound to estimate the standard deviation of the distribution, and so to estimate the width of a six-sigma interval above the best estimate (Otto et al., 2024). Datasets where the upper bound was inferred in this way are marked with an asterisk * in the figures below.

Observation-based products and models are combined into a single result in two ways. Firstly, we neglect common model uncertainties beyond the inter-model spread that is depicted by the model average, and compute the weighted average of models (dark red bar) and observations (dark blue bar): this is indicated by the magenta bar. As, due to common model uncertainties, model uncertainty can be larger than the inter-model spread, secondly, we also show the more conservative estimate of an unweighted, direct average of observations (dark blue bar) and models (dark red bar) contributing 50% each, indicated by the white box around the magenta bar in the synthesis figures.

A.4.1 Extreme rainfall

A.4.1.1 Jamaica

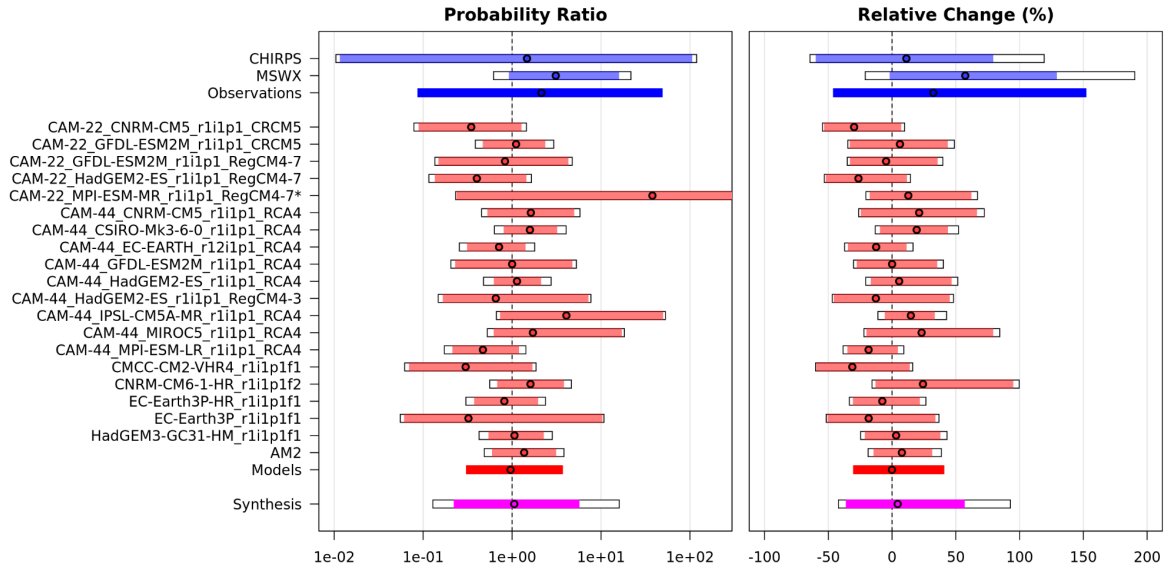

Figure A11: *Synthesised changes for a 40-year 5-day SON maximum rainfall event over Jamaica due to GMST. Changes in PR (left) and intensity (right) are shown for a historical period comparing the past 1.3°C cooler climate with the present (top row). Note: AM2 refers to the AM2.5C360 ensemble described in section A.1.2.*

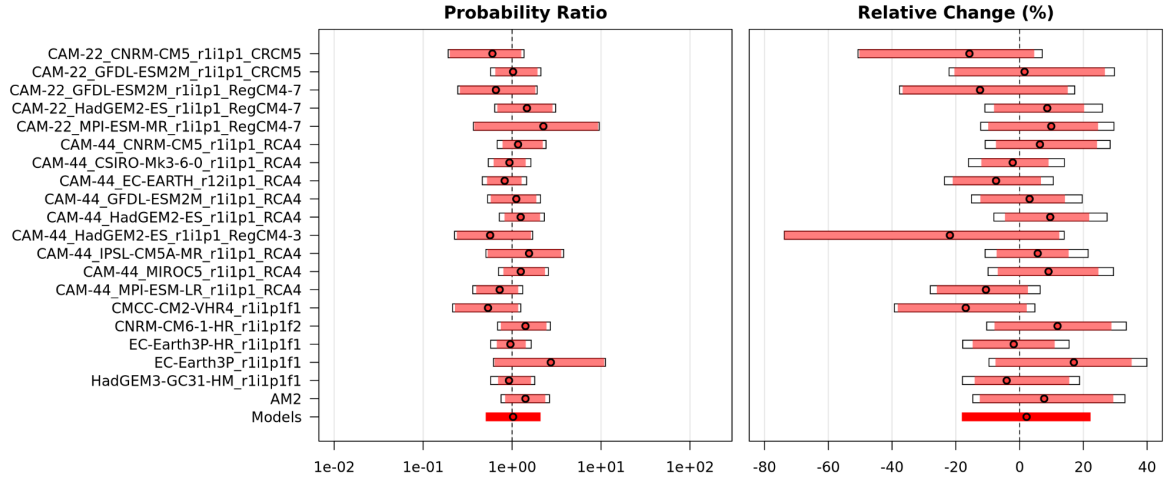

Figure A12: *Synthesised changes for a 40-year 5-day SON maximum rainfall event over Jamaica due to GMST. Changes in PR (left) and intensity (right) are shown for a historical period comparing the future 1.3°C warmer climate with the present (top row). Note: AM2 refers to the AM2.5C360 ensemble described in section A.1.2.*

A.4.1.2 Eastern Cuba

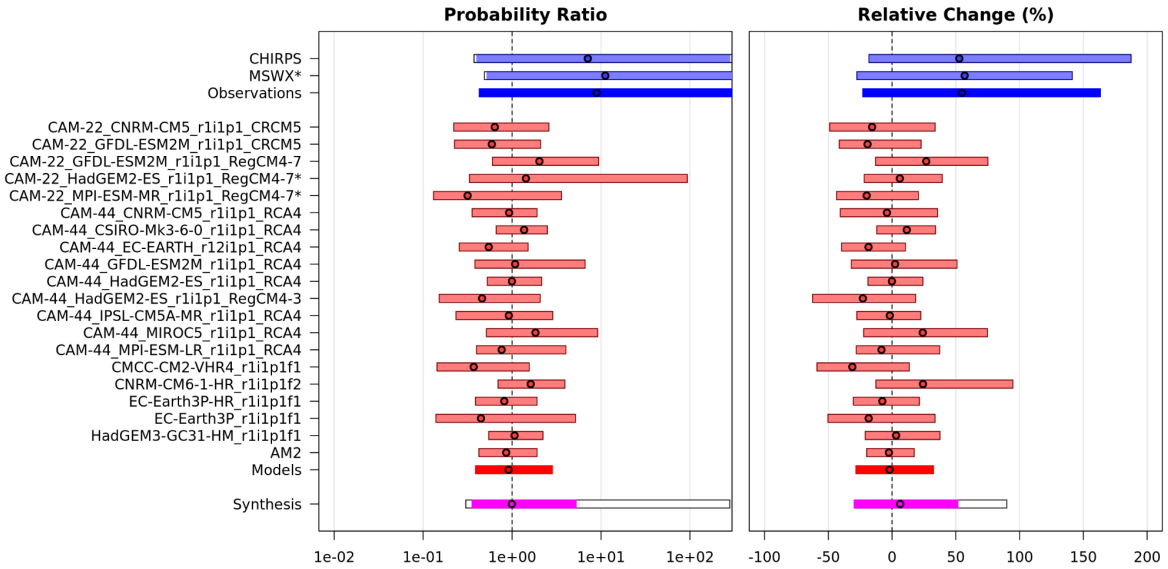

Figure A13: *Synthesised changes for a 10-year 5-day SON maximum rainfall event over eastern Cuba due to GMST. Changes in PR (left) and intensity (right) are shown for a historical period comparing the past 1.3°C cooler climate with the present (top row). Note: AM2 refers to the AM2.5C360 ensemble described in section A.1.2.*

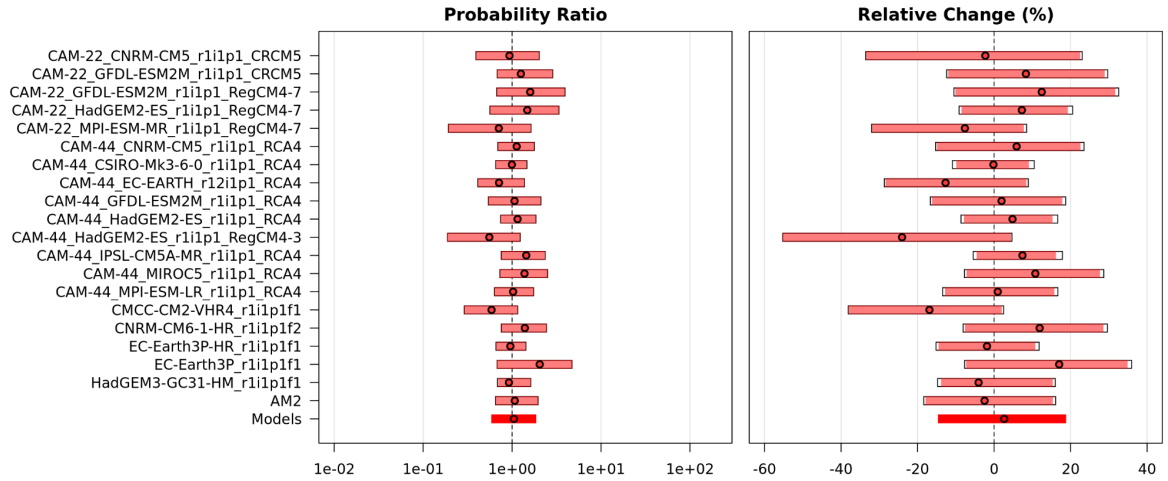

Figure A14: *Synthesised changes for a 10-year 5-day SON maximum rainfall event over eastern Cuba due to GMST. Changes in PR (left) and intensity (right) are shown for a historical period comparing the future 1.3°C warmer climate with the present (top row). Note: AM2 refers to the AM2.5C360 ensemble described in section A.1.2.*

A.4.2 Potential intensity

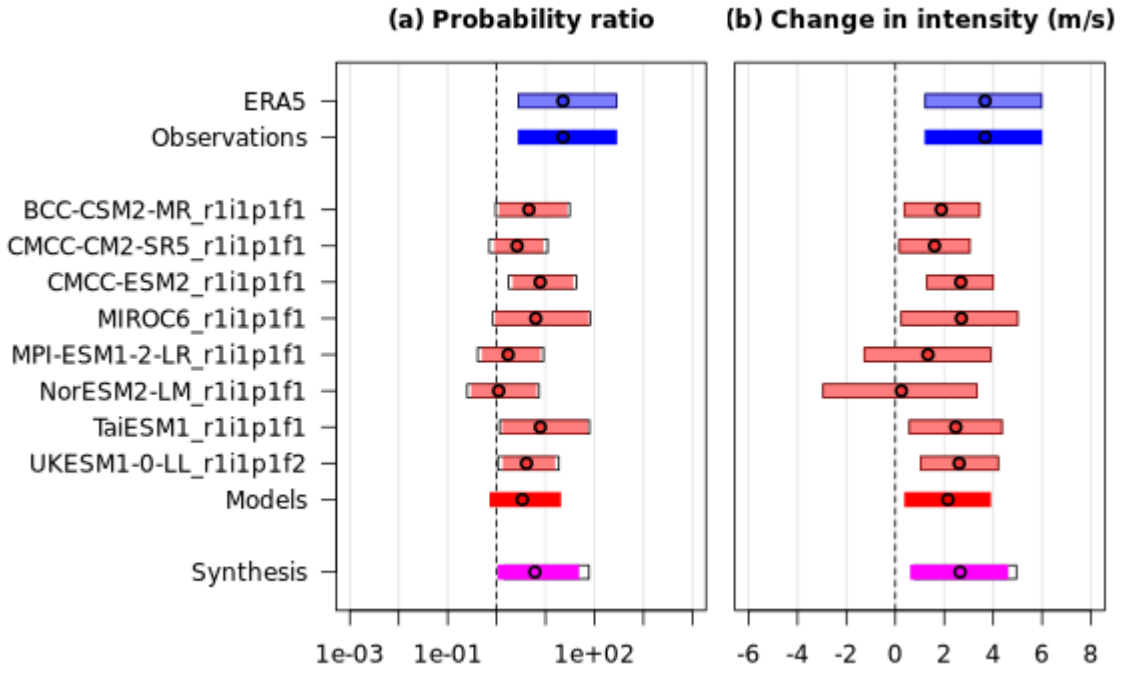

Figure A15: *Synthesised changes for a 5-year annual maximum monthly PI event over the study region due to GMST. Changes in PR (left) and intensity (right) are shown for a historical period comparing the past 1.3°C cooler climate with the present (top row).*

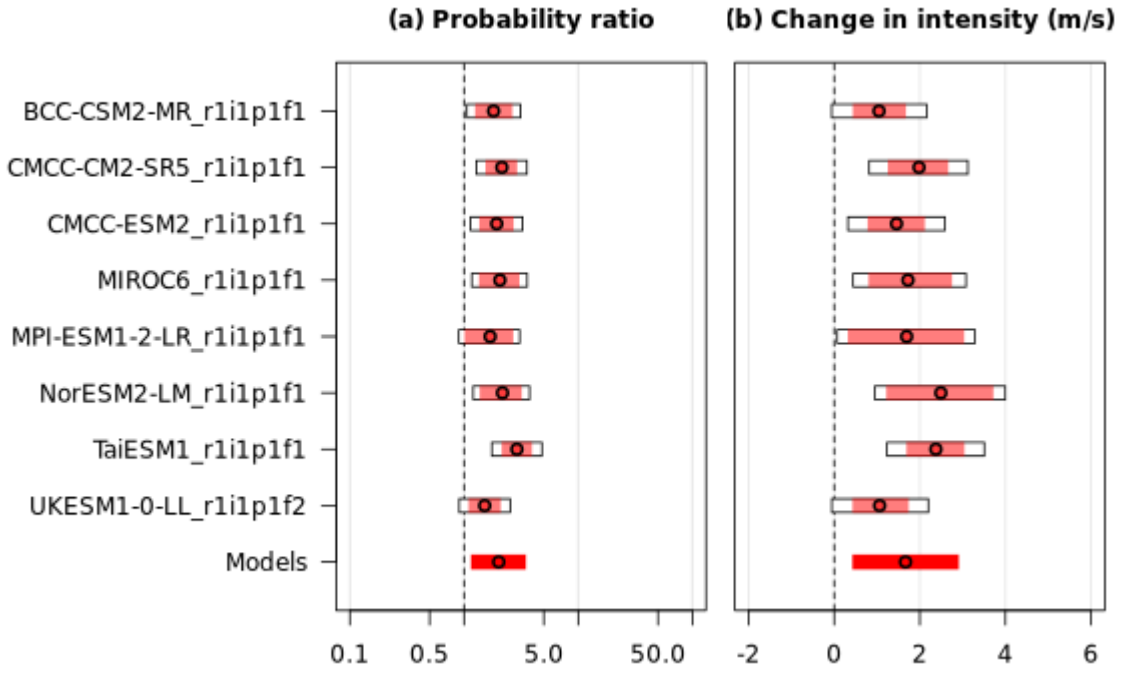

Figure A16: *Synthesised changes for a 5-year annual maximum monthly PI event over the study region due to GMST. Changes in PR (left) and intensity (right) are shown for a historical period comparing the future 1.3°C warmer climate with the present (top row).*